

Morphology and molecular phylogeny of three new deep-sea species of *Chrysogorgia* (Cnidaria, Octocorallia) from seamounts in the tropical Western Pacific Ocean

Yu Xu^{1,2,3,4}, Zifeng Zhan^{1,2,3}, Kuidong Xu^{Corresp. 1,2,3,4}

¹ Laboratory of Marine Organism Taxonomy and Phylogeny, Institute of Oceanology, Chinese Academy of Sciences, Qingdao, China

² Laboratory for Marine Biology and Biotechnology, Pilot National Laboratory for Marine Science and Technology (Qingdao), Qingdao, China

³ Center for Ocean Mega-Science, Chinese Academy of Sciences, Qingdao, China

⁴ University of Chinese Academy of Sciences, Beijing, China

Corresponding Author: Kuidong Xu
Email address: kxu@qdio.ac.cn

Three new species of *Chrysogorgia* were discovered from seamounts in the tropical Western Pacific Ocean. *Chrysogorgia dendritica* sp. nov. and *Chrysogorgia fragilis* sp. nov. were collected from the Kocebu Guyot of the Magellan Seamount chain with the water depth of 1,821 m and 1,279–1,321 m, respectively, and *Chrysogorgia gracilis* sp. nov. was collected from a seamount adjacent to the Mariana Trench with the water depth of 298 m. They all belong to the *Chrysogorgia* “group A, Spiculosae” with rods distributed in body wall and tentacles, and differ from all congeners except *C. abludo* Pante & Watling, 2012 by having a tree-shaped colony. *Chrysogorgia dendritica* sp. nov. is unique in having a monopodial stem, the 1/3L branching sequence and the amoeba-shaped sclerites at the body bases of polyps. *Chrysogorgia fragilis* sp. nov. is most similar to *C. abludo*, but differs by the regular 1/3L branching sequence and elongate skateboard-shaped scales in coenenchyme. *Chrysogorgia gracilis* sp. nov. is easily separated from congeners by the 1/4L branching sequence, the absence of sclerites in the basal body wall, and the very sparse scales in coenenchyme. Based on the phylogenetic and genetic distance analyses of mtMutS gene, all the available *Chrysogorgia* species were separated into two main groups: one includes *C. binata*, *C. cf. stellata* and *C. chryseis*, which have two or more fans emerging from a short main stem (bi- or multi-flabellate colony); the other one includes all the species with the branching patterns as a single ascending spiral, a fan (planar colony) and a tree-shaped colony. Additionally, the tree-shaped colony represents a new branching pattern in *Chrysogorgia*, and therefore we extend the generic diagnosis.

1 **Morphology and molecular phylogeny of three new deep-sea species of *Chrysogorgia***
2 **(Cnidaria, Octocorallia) from seamounts in the tropical Western Pacific Ocean**

3

4 Yu Xu^{1,2,3,4}, Zifeng Zhan^{1,2,3}, Kuidong Xu^{1,2,3,4}

5

6 ¹ Laboratory of Marine Organism Taxonomy and Phylogeny, Institute of Oceanology, Chinese
7 Academy of Sciences, Qingdao, Shandong, China

8 ² Laboratory for Marine Biology and Biotechnology, Pilot National Laboratory for Marine
9 Science and Technology (Qingdao), Qingdao, Shandong, China

10 ³ Center for Ocean Mega-Science, Chinese Academy of Sciences, Qingdao, Shandong, China

11 ⁴ University of Chinese Academy of Sciences, Beijing, China

12

13 Corresponding Author: Kuidong Xu

14 7 Nanhai Rd., Qingdao, Shandong, 266071, China

15 Email address: kxu@qdio.ac.cn

16

17 **Abstract**

18 Three new species of *Chrysogorgia* were discovered from seamounts in the tropical Western
19 Pacific Ocean. *Chrysogorgia dendritica* sp. nov. and *Chrysogorgia fragilis* sp. nov. were
20 collected from the Kocebu Guyot of the Magellan Seamount chain with the water depth of 1,821
21 m and 1,279–1,321 m, respectively, and *Chrysogorgia gracilis* sp. nov. was collected from a
22 seamount adjacent to the Mariana Trench with the water depth of 298 m. They all belong to the
23 *Chrysogorgia* “group A, Spiculosae” with rods distributed in body wall and tentacles, and differ
24 from all congeners except *C. abludo* Pante & Watling, 2012 by having a tree-shaped colony.
25 *Chrysogorgia dendritica* sp. nov. is unique in having a monopodial stem, the 1/3L branching
26 sequence and the amoeba-shaped sclerites at the body bases of polyps. *Chrysogorgia fragilis* sp.
27 nov. is most similar to *C. abludo*, but differs by the regular 1/3L branching sequence and elongate
28 skateboard-shaped scales in coenenchyme. *Chrysogorgia gracilis* sp. nov. is easily separated
29 from congeners by the 1/4L branching sequence, the absence of sclerites in the basal body wall,
30 and the very sparse scales in coenenchyme. Based on the phylogenetic and genetic distance
31 analyses of mtMutS gene, all the available *Chrysogorgia* species were separated into two main
32 groups: one includes *C. binata*, *C. cf. stellata* and *C. chryseis*, which have two or more fans
33 emerging from a short main stem (bi- or multi-flabellate colony); the other one includes all the
34 species with the branching patterns as a single ascending spiral, a fan (planar colony) and a tree-
35 shaped colony. Additionally, the tree-shaped colony represents a new branching pattern in
36 *Chrysogorgia*, and therefore we extend the generic diagnosis.

37

38 **Keywords** Anthozoa, Chrysogorgiidae, *Chrysogorgia dendritica*, *Chrysogorgia fragilis*,
39 *Chrysogorgia gracilis*, taxonomy

40

41 **Introduction**

42 The genus *Chrysogorgia* Duchassaing & Michelotti, 1864 contains 72 species distributed in the
43 world oceans, with water depths ranging from 100 m to 3860 m (Pante et al., 2012; Cairns,
44 2018; Xu et al., 2019). Three branching forms have been recognized in the colonies of the genus:
45 a single ascending spiral (clockwise or counterclockwise) producing a bottlebrush shape, a single
46 fan (planar colony) and two fans emerging from a short main stem (biflabellate colony) (Pante &
47 Watling, 2012; Cordeiro et al., 2015). Based on the shapes of rods or scales in the body wall and
48 tentacles, a rough grouping has been built for the separation of *Chrysogorgia* species. Versluys

49 (1902) divided the genus *Chrysogorgia* into three groups, which were summarized by Cairns
50 (2001) as “group A, Spiculosae”, “group B, Squamosae aberrantes”, and “group C, Squamosae
51 typicae”. Cordeiro et al. (2015) supplemented the fourth group “group D, Spiculosae aberrantes”,
52 which contains only the species *C. upsilonia* Cordeiro, Castro & Pérez, 2015.

53 While studying the benthic diversity in the tropical Western Pacific Ocean, we collected four
54 specimens of *Chrysogorgia*. Based on morphological and phylogenetic analyses, we describe
55 these specimens as three new species: *C. dendritica* sp. nov., *C. fragilis* sp. nov. and *C. gracilis*
56 sp. nov. Their genetic distances and single mutations on mtMutS as well as phylogenetic
57 relationships within *Chrysogorgia* species are discussed.

58

59 **Materials & Methods**

60

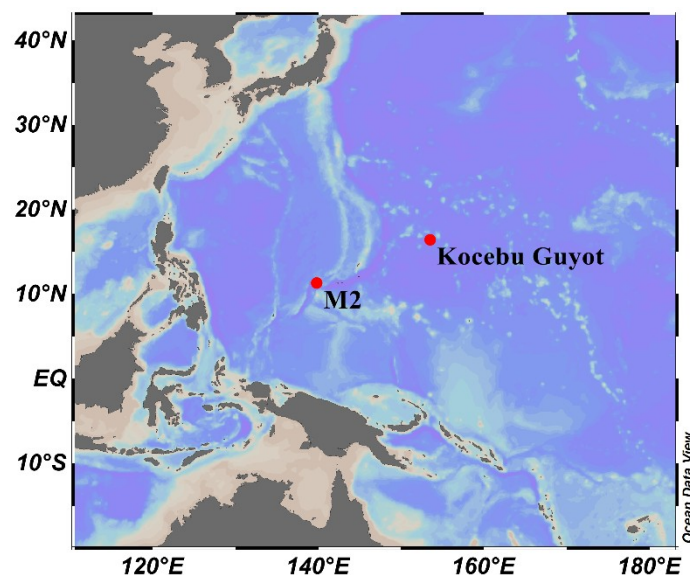
61 **Specimen collection and morphological examination**

62 Specimens were obtained by the remotely operated vehicle (ROV) *FaXian* (Discovery) from an
63 unnamed seamount (temporarily named as M2) adjacent to the Mariana Trench and the Kocebu
64 Guyot in the Magellan Seamounts in the tropical Western Pacific Ocean during the cruises of the
65 R/V *KeXue* (Science) in 2016 and 2018 (Fig. 1). These specimens were photographed *in situ*
66 before sampled, photographed on board and then stored in 75% ethanol after collection. Some
67 branches were detached and stored at -80°C for molecular analysis.

68 The morphological terminology used follows Bayer et al. (1983). The general morphology
69 and anatomy were examined by using a stereo dissecting microscope. The sclerites of the polyps
70 and branches were isolated by digestion of the tissues in sodium hypochlorite, and then were
71 washed with deionized water repeatedly. Polyps and sclerites were air-dried and mounted on
72 carbon double adhesive tape and coated for the Scanning Electron Microscope (SEM) to
73 investigate their structure. SEM scans were obtained and the optimum magnification was chosen
74 for each kind of sclerites by using TM3030Plus SEM.

75 The type specimens of the three new species have been deposited in the Marine Biological
76 Museum of Chinese Academy of Sciences (MBMCAS) at Qingdao, China.

77



78

79 **Figure 1 Sampling sites on a seamount (M2) adjacent to the Mariana Trench and the**
80 **Kocebu Guyot in the Western Pacific Ocean.**

81

82 **DNA extraction and sequencing**

83 Total genomic DNA was extracted from the polyps of each specimen using the TIANamp Marine
84 Animal DNA Kit (Tiangen Bio. Co., Beijing, China) following the manufacturer's instructions.
85 PCR amplification for the mitochondrial genomic region 5'-end of the DNA mismatch repair
86 protein - *mutS* - homolog (mtMutS) was conducted using primers AnthoCorMSH (5'-
87 AGGAGAATTATTCTAAGTATGG-3'; [Herrera et al., 2010](#)) and Mut-3458R (5'-
88 TSGAGCAAAGCCACTCC-3'; [Sánchez et al., 2003](#)). PCR reactions were performed using I-
89 5™ 2 × High-Fidelity Master Mix DNA polymerase (TsingKe Biotech, Beijing, China). The
90 amplification cycle conditions were as follow: denaturation at 98°C for 2 min, followed by 32
91 cycles of denaturation at 98°C for 20 s, annealing at 50°C for 20 s, extension at 72°C for 15 s,
92 and a final extension step at 72°C for 2 min. PCR purification and sequencing were performed by
93 TsingKe Biological Technology (TsingKe Biotech, Beijing, China).

94

95 **Genetic distance and phylogenetic analyses**

96 The mtMutS may be the most variable mitochondrial gene in octocorals ([Herrera et al., 2010](#);
97 [McFadden et al., 2011](#); [Li et al., 2017](#)), and we selected this marker for molecular identification
98 and phylogenetic analyses. All the available mtMutS sequences of *Chrysogorgia* spp. and the out-
99 group species from related chrysogorgiid genera were downloaded from GenBank. The
100 sequences from duplicate isolates or without associated publications or named *Chrysogorgia* sp.
101 or containing sequencing errors (marked with “n” or “y” in the original sequences) were omitted
102 from the molecular analyses. To correct possible mistakes, all the selected sequences were
103 visually inspected, and translated to amino acids (AA) to insure all the AA sequences not
104 including stop codons and suspicious substituteions. The nucleotide and AA sequences were
105 aligned using MAFFT v.7 ([Katoh & Standley, 2013](#)) with the G-INS-i algorithm. With the
106 guidance of the AA alignment, the nucleotide alignment was refined using BioEdit v7.0.5 (Hall,
107 1999), and only the nucleotide alignment was used in the subsequent analyses. Genetic distances,
108 calculated as uncorrected “p” distances within each species and among species, were estimated
109 using MEGA 6.0 ([Tamura et al., 2013](#)).

110 For the phylogenetic analyses, only one sequence was randomly selected from the
111 conspecific sequences without genetic divergence (see Table 2). The evolutionary model GTR+G
112 was the best-fitted model for mtMutS, selected by AIC as implemented in jModeltest2 ([Darriba
113 et al., 2012](#)). Maximum likelihood (ML) analysis was carried out using PhyML-3.1 ([Guindon et
114 al., 2010](#)). For the ML bootstraps, we consider values < 70% as low, 70–94% as moderate and ≥
115 95% as high following Hillis & Bull (1993). Node support came from a majority-rule consensus
116 tree of 1 000 bootstrap replicates. Bayesian inference (BI) analysis was carried out using
117 MrBayes v3.2.3 ([Ronquist & Huelsenbeck, 2003](#)) on CIPRES Science Gateway. Posterior
118 probability was estimated using four chains running 10 000 000 generations sampling every 1
119 000 generations. The first 25% of sampled trees were considered burn-in trees. Convergence was
120 assessed by checking the standard deviation of partition frequencies (< 0.01), the potential scale
121 reduction factor (ca. 1.00), and the plots of log likelihood values (no obvious trend was observed

122 over time). For the Bayesian posterior probabilities, we consider values < 0.95 as low and ≥ 0.95
123 as high following Alfaro et al. (2003). The GenBank accession numbers of the mtMutS sequences
124 were listed next to the species names in the phylogenetic tree (Fig. 9).

125

126 **ZooBank registration**

127 The electronic version of this article in Portable Document Format (PDF) will represent a
128 published work according to the International Commission on Zoological Nomenclature (ICZN),
129 hence the new names contained in the electronic version are effectively published under that
130 Code from the electronic edition alone. This published work and the nomenclatural acts it
131 contains have been registered in ZooBank, the online registration system for the ICZN. The
132 ZooBank Life Science Identifiers (LSIDs) can be resolved and the associated information viewed
133 through any standard web browser by appending the LSID to the prefix <http://zoobank.org/>. The
134 LSID for this publication is: urn:lsid:zoobank.org:pub:00D5E053-EFF8-4142-8D16-
135 AAFC17D028E2. The online version of this work is archived and available from the following
136 digital repositories: PeerJ, PubMed Central, and CLOCKSS.

137

138 **Results**

139

140 **Class Anthozoa Ehrenberg, 1834**

141 **Subclass Octocorallia Haeckel, 1866**

142 **Order Alcyonacea Lamouroux, 1812**

143 **Suborder Calcaxonia Grasshoff, 1999**

144 **Family Chrysogorgiidae Verrill, 1883**

145 **Genus *Chrysogorgia* Duchassaing & Michelotti, 1864**

146

147 ***Chrysogorgia dendritica* sp. nov. (Figs. 2–4; Table 1)**

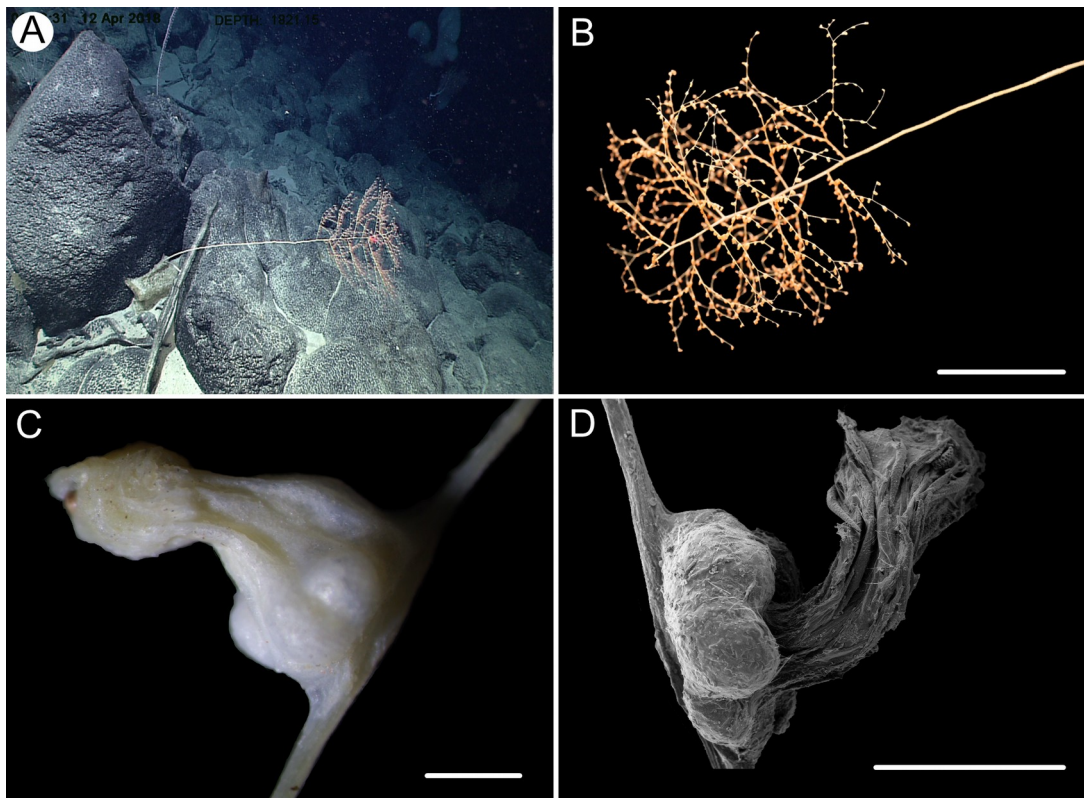
148 urn:lsid:zoobank.org:act:F0050AD3-9E65-4B03-8D26-2C687018DCAD

149

150 **Holotype.** MBM286354, station FX-Dive 178 (17°20.18'N, 152°41.85'E), Kocebu Guyot, depth
151 1,821 m, 12 April 2018. GenBank accession number: MN510469.

152 **Diagnosis.** *Chrysogorgia* “group A, Spiculosae” with a long monopodial stem and a branching
153 part on the top. Branching sequence 1/3L. Branches nearly perpendicular to stem, subdivided
154 dichotomously. Polyps with a long neck and an expanded base. Rods and spindles in tentacles
155 and polyp neck coarse with many warts. Scales at polyp body base flat and amoeba-shaped.
156 Scales in coenenchyme thin with irregular edges.

157



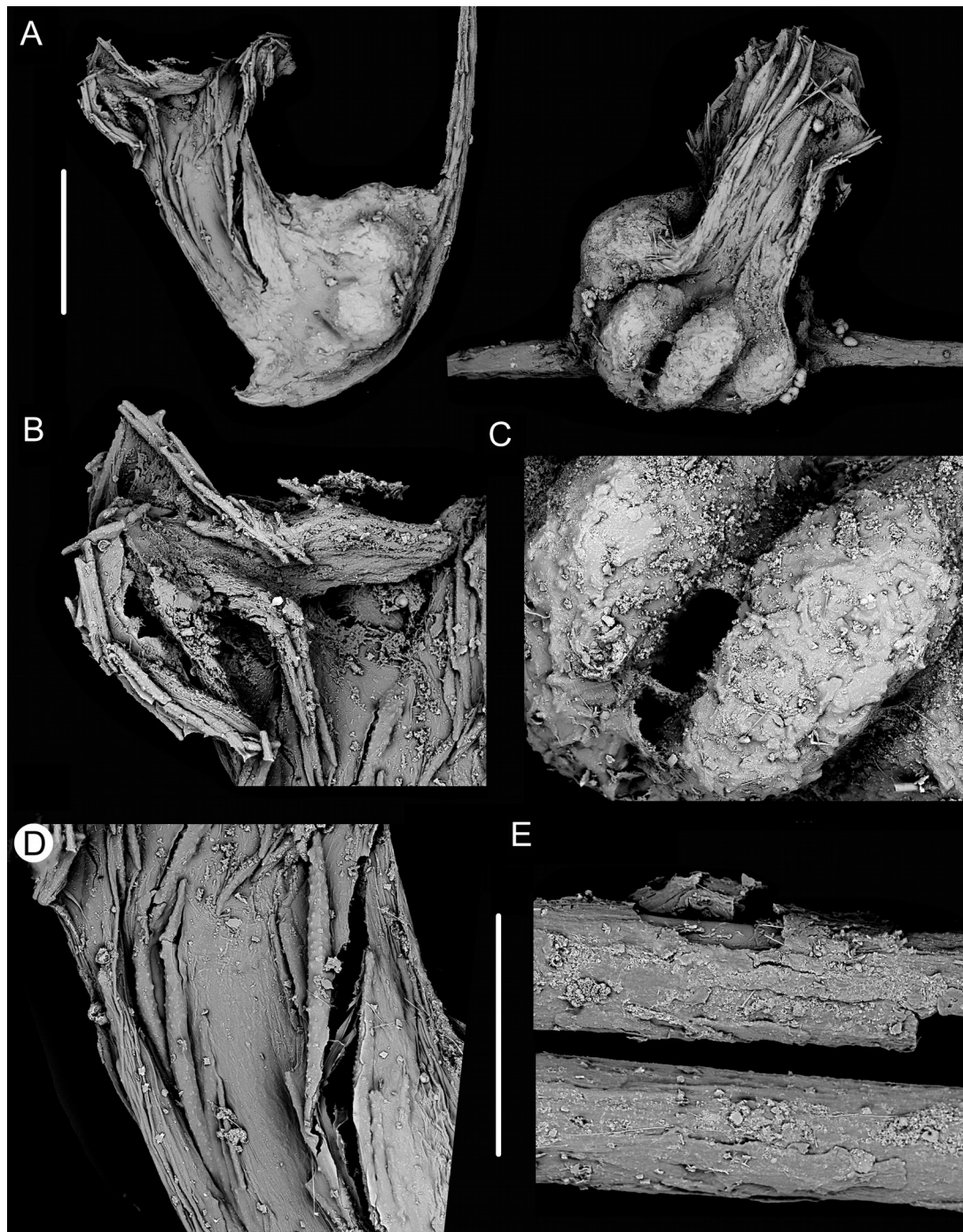
158

159 **Figure 2** The external morphology and polyps of *Chrysogorgia dendritica* sp. nov. (A) The
 160 holotype *in situ*; (B) The holotype immediately after collection; (C) A single polyp under light
 161 microscope; (D) Single polyp under SEM. Scale bars: 10 cm (B); 1 mm (C, D).

162

163 **Description.** Specimen about 57 cm long with the holdfast not recovered. Colony tree-shaped,
 164 composed of a 36 cm long, straight and unbranched stem and a 21 cm long branched part with
 165 branching sequence 1/3L. Stem surface almost smooth with a strong golden metallic luster, about
 166 2 mm in diameter at base (Figs. 2A, 2B). Branches subdivided dichotomously, up to seventh
 167 order, most broken after collection. Distance between adjacent branches 16–22 mm, and
 168 orthostiche interval 50–55 mm. First branch internodes 15–20 mm long, with the terminal
 169 branchlets up to 50 mm. Polyps with a long neck and an expanded base, about 3 mm long and 2
 170 mm wide at bases, composed of one or two on the first internodes, one to five in middle
 171 internodes, and up to six in terminal branchlets (Figs. 2C, 2D). No polyps on main axis
 172 internodes. Golden eggs often occurred at the expanded bases.

173



174
175
176
177
178
179

Figure 3 Polyps and branches of *Chrysogorgia dendritica* sp. nov. under SEM. (A) A terminal polyp and a middle polyp; (B) The tentacles with rods; (C) The basal body with scales; (D) The neck with rods and spindles; (E) The coenenchyme with scales. Scale bars: 1 mm (A); 500 μ m (B–E at the same scale).



180
181 **Figure 4** Sclerites of *Chrysogorgia dendritica* sp. nov. (A) Sclerites of the polyp neck and
182 tentacles; (B) Sclerites at the body base; (C) Sclerites in coenenchyme. Scale bars: 200 μm (A),
183 100 μm (B, C, at the same scale).
184

185

Spindles and rods longitudinally arranged in the long polyp neck and the rachis of tentacles,

186 slender with many small warts on surface, usually slightly curved and occasionally branched,
187 measuring $77\text{--}800 \times 15\text{--}56 \mu\text{m}$ (Figs. 3, 4A). Scales at body base flat and amoeba-shaped, with
188 irregular edges, measuring $69\text{--}248 \times 11\text{--}79 \mu\text{m}$ (Figs. 3C, 4B). Scales of coenenchyme sparse,
189 flat and lobed with irregular edges, measuring $68\text{--}268 \times 10\text{--}70 \mu\text{m}$ (Figs. 3E, 4C).

190 **Type locality.** Kocebu Guyot in the Magellan Seamount chain with water depth of 1,821 m.

191 **Etymology.** The Latin adjective *dendriticus* (dendritic) refers to the dendritic shape of the colony.

192 **Distribution and Habitat.** Found only on the Kocebu Guyot, where the colony attached to a
193 dried sponge (Fig. 2A). The water temperature was about 2.31°C and the salinity about 35.8 psu.

194 **Remarks.** *Chrysogorgia dendritica* sp. nov. has a monopodial stem, which makes it appear to be
195 a member of the chrysogorgiid genus *Metallogorgia* Versluys, 1902. However, the new species is
196 characterized by a series of features matching the genus *Chrysogorgia* Duchassaing & Michelotti,
197 1864. These include the soft branches, dichotomously subdivided branches not forming a
198 sympodia, relatively large polyp with an expanded base and a narrow neck, and differentiated
199 coenenchyme. Our phylogenetic analysis (see below) supports this assignment as well.

200 *Chrysogorgia dendritica* sp. nov. is distinctly different from congeners by its unique monopodial
201 stem and the amoeba-shaped sclerites at the body bases.

202

203 ***Chrysogorgia fragilis* sp. nov.** (Figs. 5 and 6; Table 1)

204 urn:lsid:zoobank.org:act:562CFDA7-88F5-4D81-8FE5-BDE1F56A3EEC

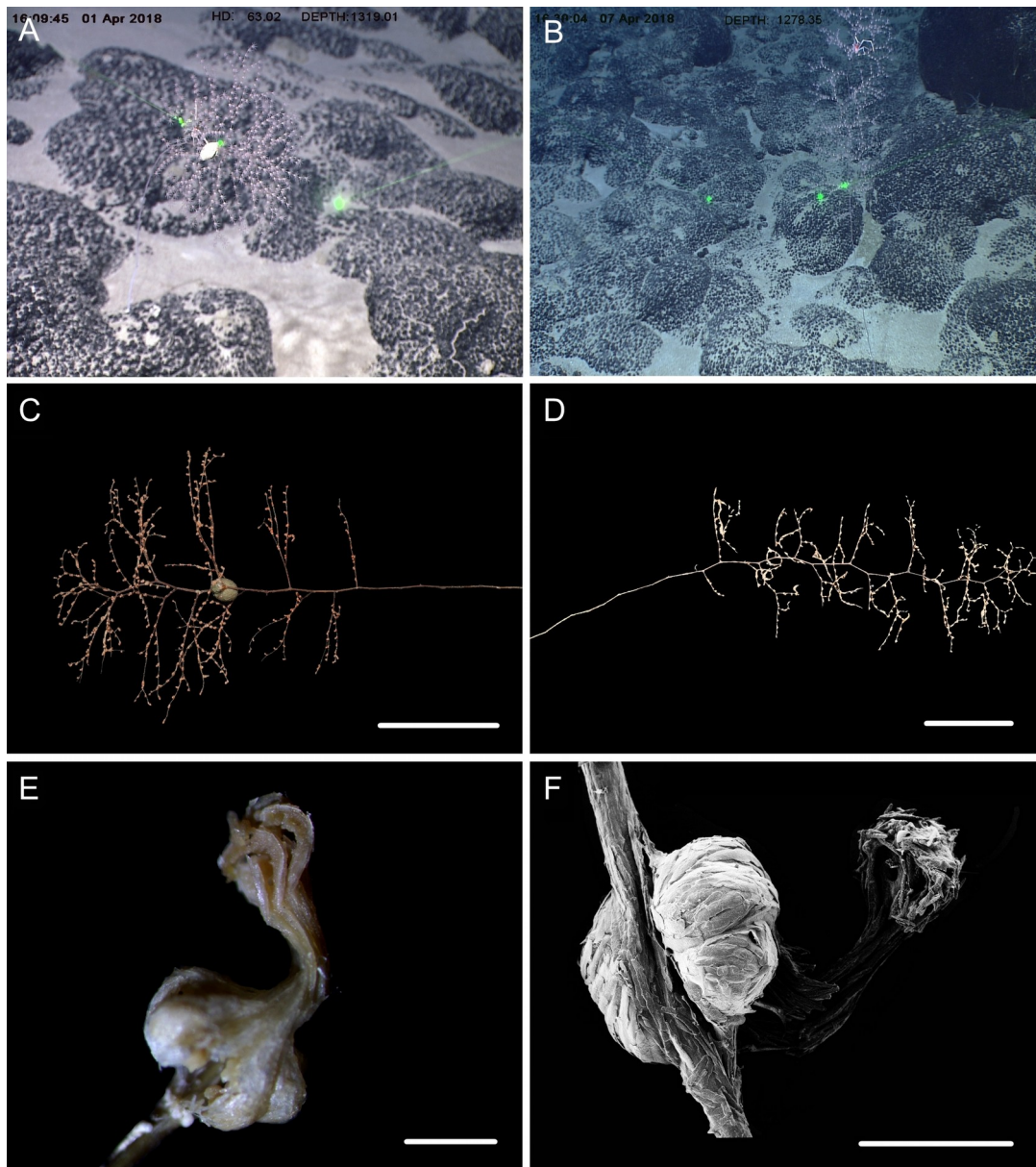
205

206 **Holotype.** MBM286351, station FX-Dive 172 ($17^\circ23.64'\text{N}$, $153^\circ6.07'\text{E}$), Kocebu Guyot, depth
207 1,321 m, 1 April 2018. GenBank accession number: MN510470.

208 **Paratype.** MBM286352, station FX-Dive 173 ($17^\circ28.12'\text{N}$, $153^\circ10.07'\text{E}$), Kocebu Guyot, depth
209 1,279 m, 7 April 2018.

210 **Diagnosis.** *Chrysogorgia* “group A, Spiculosae” with a long unbranched stem and a sympodial
211 branching part with 1/3L branching sequence on the top. Branches subdivided dichotomously, up
212 to fifth order. Polyps with an expanded base and a slender neck. Rods and spindles of the polyp
213 neck and tentacles long and coarse, with many warts on surface. Scales at polyp body base
214 elongated and thick, rarely branched. Scales in coenenchyme flat and elongated with irregular
215 edges.

216



217

218

219 **Figure 5** The external morphology and polyps of *Chrysogorgia fragilis* sp. nov. (A) The

220

221 holotype *in situ*. Laser dots spaced at 33 cm used for measuring dimensions; (B) The paratype *in*

222

223 *in situ*; (C) The holotype immediately after collection; (D) The paratype after fixation; (E) A single

224

225 polyp under light microscope; (F) A single polyp under SEM. Scales bars: 10 cm (C, D); 1 mm

226

227 (E, F).

228

229 **Description.** Specimen of holotype about 55 cm in height excluding the holdfast. Colony tree-

230

231 shaped, composed of a sympodial branching part on the top and a fragile, slender and unbranched

232 branches up to 75 mm. Polyps with a long neck and an expanded body base, 2–4 mm long, 1–2
233 mm wide at base, with the neck up to 2 mm long and less than 1 mm wide (Figs. 5E, 5F). Up to
234 two polyps on the first internodes, two to four in middle internodes, up to ten in terminal
235 branchlets. No polyp on main axis internodes. Golden eggs present in expanded body bases.
236 Polyps pink immediately after collection, color gradually faded in alcohol.

237 Spindles and rods longitudinally arranged in the neck and tentacles, slender with many small
238 warts on surface, rarely branched, measuring $105\text{--}600 \times 14\text{--}62 \mu\text{m}$ (Figs. 5F, 6A). Scales at base
239 of expanded polyp body elongated with a few warts and irregular edges, sometimes branched,
240 thicker and wider than those in coenenchyme, measuring $144\text{--}551 \times 34\text{--}106 \mu\text{m}$ (Fig. 6B). Scales
241 of coenenchyme flat and elongate, skateboard-shaped, rarely with distinctly irregular edges,
242 measuring $122\text{--}435 \times 28\text{--}83 \mu\text{m}$ (Fig. 6C).

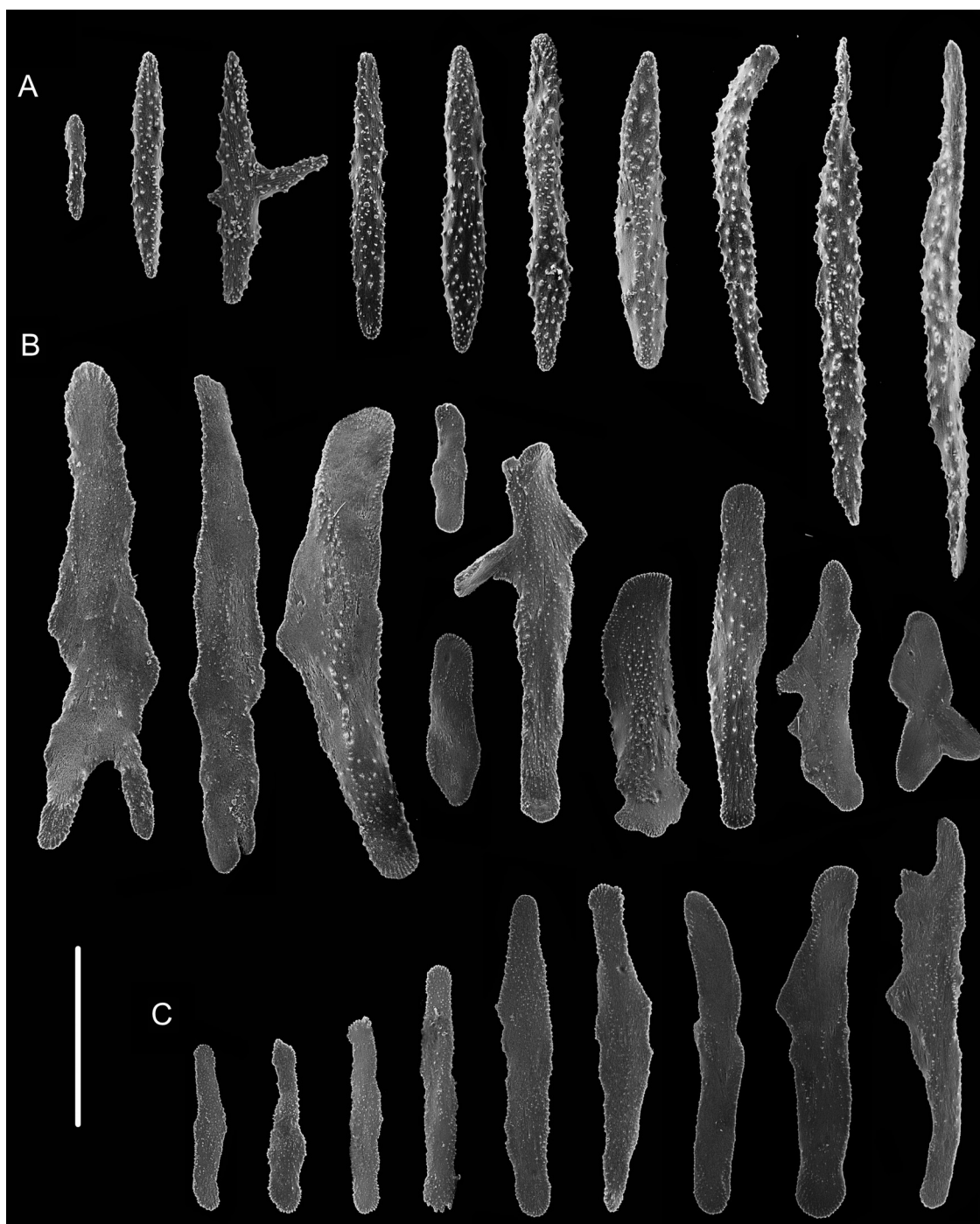
243 **Variation of Paratype.** Specimen 65 cm in height with unbranched stem about 35 cm long and 1
244 mm across at base (Fig. 4D). Branching part relatively longer and more zigzagging.

245 **Type locality.** Kocebu Guyot in the Magellan Seamount chain with water depths of 1,279–1,321
246 m.

247 **Etymology.** The Latin adjective *fragilis* (fragile) refers to the fragile stem and branches of the
248 species.

249 **Distribution and habitat.** Found only on the Kocebu Guyot in the Magellan Seamount chain.
250 Colonies attached to rocky substrate. The holotype was attached with an egg-shaped structure and
251 the paratype with an individual of the crustacean genus *Galathea* Fabricius, 1793 (Figs. 5A, 5B).
252 The water temperature was about 3.2°C and the salinity about 35.8.

253 **Remarks.** *Chrysogorgia fragilis* sp. nov. belongs to the “group A, Spiculosae” with an unusual
254 branching sequence of 1/3L, with which it is similar to *Chrysogorgia midas* Cairns, 2018 and *C.*
255 *dendritica* sp. nov. However, the new species differs distinctly from *C. midas* Cairns, 2018 by the
256 tree-shaped colony (vs. bottlebrush-shaped), wider orthostiche interval (50–65 mm vs. 12–18
257 mm), larger polyps (2.0–4.0 mm vs. 1.1 mm), and the presence of various shapes of scales at the
258 body bases (vs. absence). *Chrysogorgia fragilis* sp. nov. is also similar to *C. abludo* Pante &
259 Watling, 2012 and *C. averta* Pante & Watling, 2012, two species found in the north-western
260 Atlantic Ocean, in possessing the wide orthostiche interval and long and straight unbranched
261 stem. However, the new species is easily separated from *C. averta* by the tree-shaped colony (vs.
262 bottlebrush-shaped). It differs from *C. abludo* by the regular 1/3L branching sequence (vs.
263 irregular) and elongate skateboard-shaped scales in coenenchyme (vs. small rugged scales) (Table
264 1). *Chrysogorgia fragilis* sp. nov. differs from *C. dendritica* sp. nov. by a sympodial branching
265 part (vs. monopodial) and relatively regular scales at the body bases (vs. amoeba-shaped).
266



267
 268 **Figure 6** Sclerites of *Chrysogorgia fragilis* sp. nov. (A) Sclerites of the polyp neck and
 269 tentacles; (B) Sclerites at the expanded polyp body base; (C) Sclerites in coenenchyme. Scale bar:
 270 200 μm (all at the same scale).
 271

272 **Table 1** Morphological comparisons between *C. averta*, *C. abludo*, *C. dendritica* sp. nov., *C.*
 273 *fragilis* sp. nov. and *C. gracilis* sp. nov.

Characters/species	<i>C. averta</i>	<i>C. abludo</i>	<i>C. fragilis</i> sp. nov.	<i>C. dendritica</i> sp. nov.	<i>C. gracilis</i> sp. nov.
Group type	A	A	A	A	A
Colony shape	bottlebrush-	tree-shaped	tree-shaped	tree-shaped	tree-shaped

	shaped				
Branching sequence	3/8L	1/3, 1/4L, irregular	1/3L	1/3L	1/4L
Interbranch distance (mm)	9–13	4.3–15.0	15–22	16–22	2.0–4.5
Orthostiche interval (mm)	75–78	No data	50–65	50–55	11–16
First branch internode (mm)	13–19	6.1–16.0	15–22	15–20	3–7
Polyps on internodes	0–2	1–2	0–4	1–5	1–10
Polyps on terminal branchlets	1–3	1–6	1–10	1–6	3–20
Polyps height (mm)	1.1–1.9	0.8–2.2	2.0–4.0	3.0	0.9–1.5
Sclerites in coenenchyme (µm)	rods and scales	small rugged scales	elongate skateboard-shaped scales	flat and lobed scales	elongated scales with smooth surface and edges
Sclerites in body wall (µm)	scales and rods	scales and rods	scales, rods and spindles	scales, rods and spindles	scales and rods
Sclerites in tentacles (µm)	rods	rods	rods	rods	scales and rods
Distribution	North Atlantic	North Atlantic	Western Pacific	Western Pacific	Western Pacific
References	Pante & Watling 2012	Pante & Watling 2012	Present study	Present study	Present study

274

275 ***Chrysogorgia gracilis* sp. nov.** (Figs. 7, 8; Table 1)276 [urn:lsid:zoobank.org:act:F557CE43-D43C-4E5F-86C1-3EFE330A9443](https://doi.org/10.121101/zoobank.org/act:F557CE43-D43C-4E5F-86C1-3EFE330A9443)

277

278 **Holotype:** MBM286350, station FX-Dive 57 (11°18.34'N, 139°21.43'E), an unnamed seamount
279 (temporarily named as M2) adjacent to the Mariana Trench, depth 298 m, 23 March 2016.

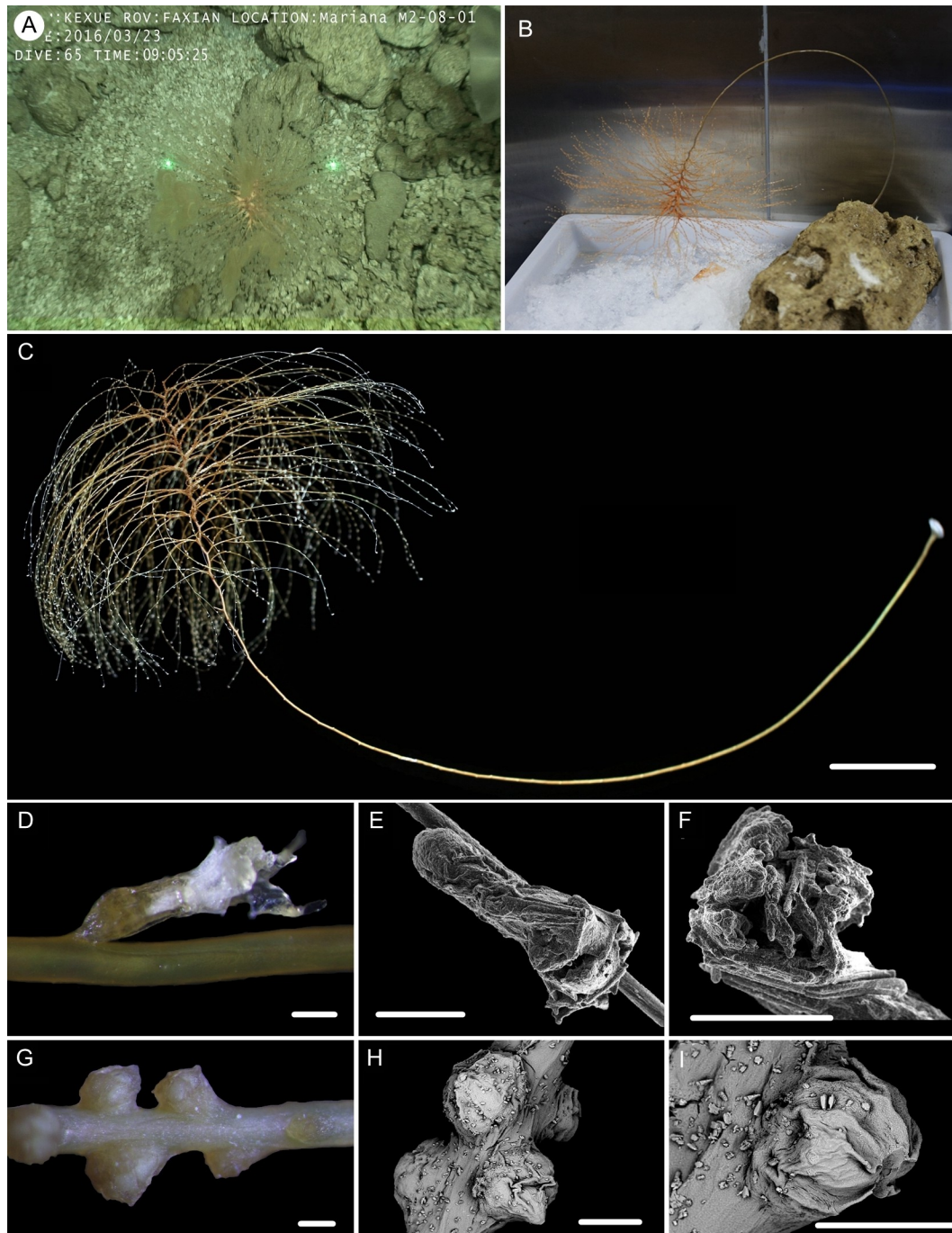
280 GenBank accession number: MN510472.

281 **Diagnosis:** *Chrysogorgia* “group A, Spiculosae” with a long unbranched stem and a sympodial
282 branching part emanating in a regular 1/4L spiral on the top. Stem and branches slender, with
283 branches subdivided dichotomously. Terminal branchlets gracile and somewhat whip-like. Polyps
284 small and thin, no more than 1.5 mm long, located on one side of branches. Rods and rod-like
285 scales slender and abundant in tentacles and at the bases of tentacles. No sclerites at polyp body
286 base. Scales elongated, rare to absent in coenenchyme. Mesozooids dense along the internodes of
287 top stem and the bases of branches.

288 **Description.** Specimen orange to reddish after collection, became yellow in alcohol, about 51.8
289 cm long (Figs. 7B, 7C). Stem and branches golden with slightly glaucous metallic luster. Colony
290 tree-shaped. Unbranched stem curved, up to 40.5 cm in arc length and 1.0–2.9 mm in diameter,
291 emanating in regular 1/4L spiral on the top of a tall (Fig. 7C). Holdfast small and rounded, about
292 9.8–12.5 mm in diameter. Distance between adjacent branches in stem 2.0–4.5 mm long and
293 orthostiche interval 11–16 mm. The first branch internodes 3–7 mm. Branches subdivided 2–7
294 times and the angle between bifurcating branches particularly obtuse: 18°–62°. Terminal
295 branchlets slender, usually whip-like, up to 90 mm long.

296 Polyps translucent, 0.9–1.5 mm long, 0.2–0.4 mm wide, uniserial spaced 2–5 mm on the
297 branches by one side, with angle random to the branches. Polyp body base golden, without

298 sclerites (Fig. 7D). Tentacles up to 1.0 mm in length, became white in alcohol. Three to 20
 299 polyps on terminal branchlets and up to ten polyps in branch internodes. Axial internodal polyps
 300 not observed in the stem, where dense mesozoids occurred along the internodes of the stem and
 301 branch bases. Mesozoids bud-like shaped, orange in situ and yellowish in alcohol, without
 302 sclerites, about 0.3–0.5 mm wide and up to 0.4 mm high (Figs. 7A, 7G–7I).
 303



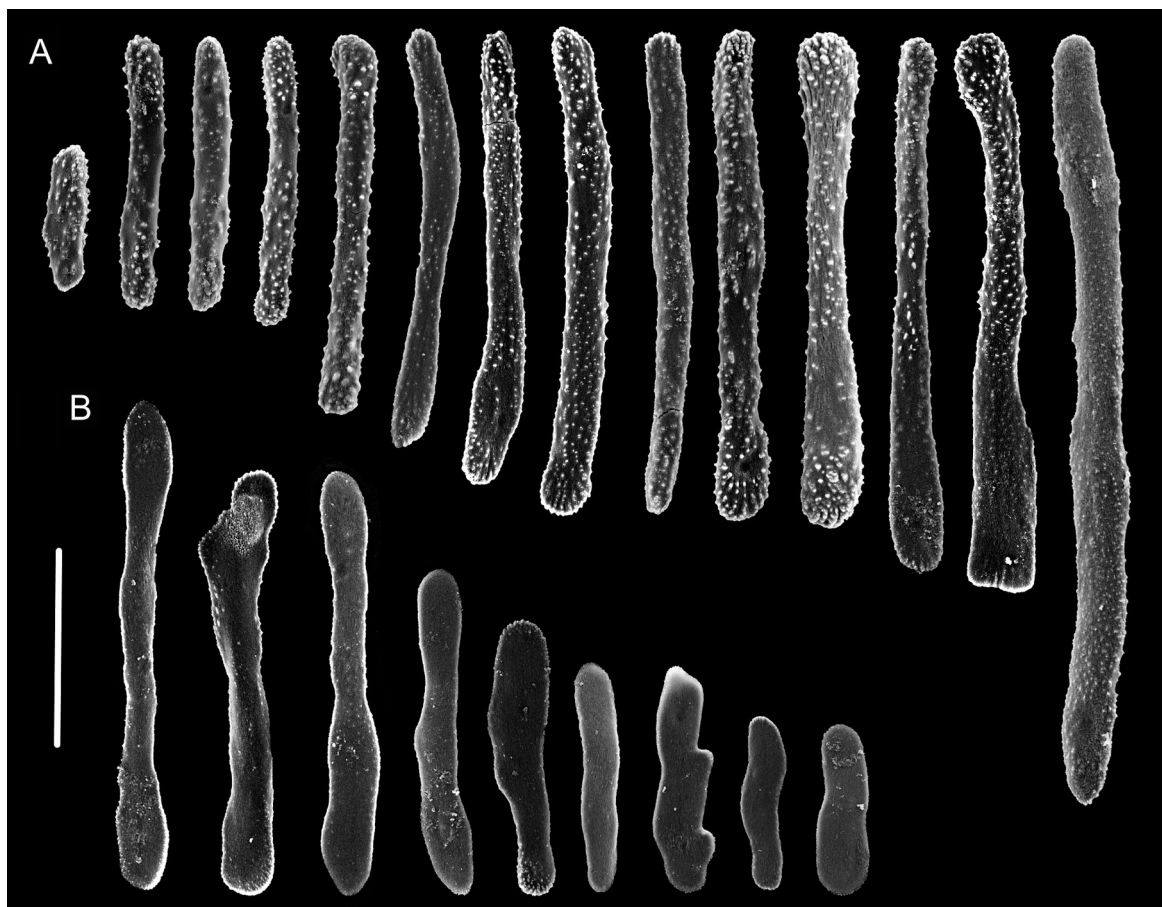
304
 305 **Figure 7** The external morphology and polyps of the holotype of *Chrysogorgia gracilis* sp.
 306 **nov.** (A–C) The holotype *in situ* (A) and after collection (B) and fixation (C); Laser dots spaced
 307 at 33 cm used for measuring dimensions; (D) A single polyp under light microscope; (E) A single
 308 polyp under SEM; (F) Tentacles under SEM; (G) Mesozoids at the base of branch under light

309 microscope; (H) Four mesozooids under SEM; (I) A single mesozooid under SEM. Scales bars:
 310 5cm (C), 300 μm (D–I).

311

312 Coenenchyme in branches with a thin pellucid and calcareous layer in outside of the central
 313 axis, sometimes with regular scales oriented along branches or without scales on branches. Scales
 314 elongated with smooth surface and edges, occasionally with finely serrated edges, usually
 315 becoming narrow in middle, rare to absent in coenenchyme, measuring 50–250 \times 12–38 μm (Fig.
 316 8B). Rods and rod-like scales slender, sometimes one end flat and the other end cylindric, mostly
 317 aggregated in the joints between the tentacles and bodies, or longitudinally along the back of the
 318 tentacles, with dentate projections at one or both ends and coarse, granular warts on surface,
 319 measuring 90–450 \times 15–20 μm (Figs. 7E, 7F, 8A). All sclerites colorless.

320



321

322 **Figure 8** Sclerites of *Chrysogorgia gracilis* sp. nov. (A) Sclerites in tentacles and at the bases of
 323 tentacles; (B) Sclerites in coenenchyme. Scales bars: 100 μm (all at the same scale).

324

325 **Type locality.** An unnamed seamount (temporarily named as M2) adjacent to the Mariana Trench
 326 with water depths of 298 m.

327 **Etymology.** The Latin adjective *gracilis* (gracile) refers to the gracile stem and branches of this
 328 species.

329 **Distribution and Habitat.** Found only on the M2 seamount adjacent to the Mariana Trench.
 330 Colony attached to a rocky substrate with a small holdfast (Fig. 7A).

331 **Remarks.** Among the species possessing 1/4L branching sequence and rods in tentacles, *C.*
332 *gracilis* sp. nov. mostly resembles *C. pyramidalis* Kükenthal, 1908 in the same branching
333 division and similar length, soft and translucent polyp's body, and the very rare sclerites in
334 coenenchyme (Kükenthal, 1908; Kinoshita, 1913; Cairns, 2001). However, *C. gracilis* sp. nov.
335 differs from *C. pyramidalis* by its distinctly longer and unbranched stem, more slender rods with
336 lobed or irregular round ends, nearly smooth and elongated scales in coenenchyme, and the
337 presence of mesozooids (Kükenthal, 1908; Kinoshita, 1913). Compared with congeners,
338 *Chrysogorgia gracilis* sp. nov. possesses much thinner and smaller polyps, where no sclerites
339 occur at the bases, and rare to absent sclerites in coenenchyme. In contrast, both the polyp body
340 wall and coenenchyme are usually composed of numerous sclerites in other species of
341 *Chrysogorgia*.

342 The specimen collected is characteristic in having numerous yellowish mesozooids on the
343 stem internodes and the bases of branches (Figs. 7G–7I). The mesozooids in this species are
344 distinguished from the nematozooids or cnidae existed in some species of *Chrysogorgia* and
345 *Iridogorgia* Verrill, 1883 (Kinoshita, 1913; Deichmann, 1936; Watling, 2007) in size, shape and
346 distribution. The nematozooids are a kind of small protuberances or verrucae distributed on the
347 surface of polyps and coenenchyme on branches, while the mesozooids are similar to polyps in
348 width and are independent on the surface of branches (Fig. 7A).

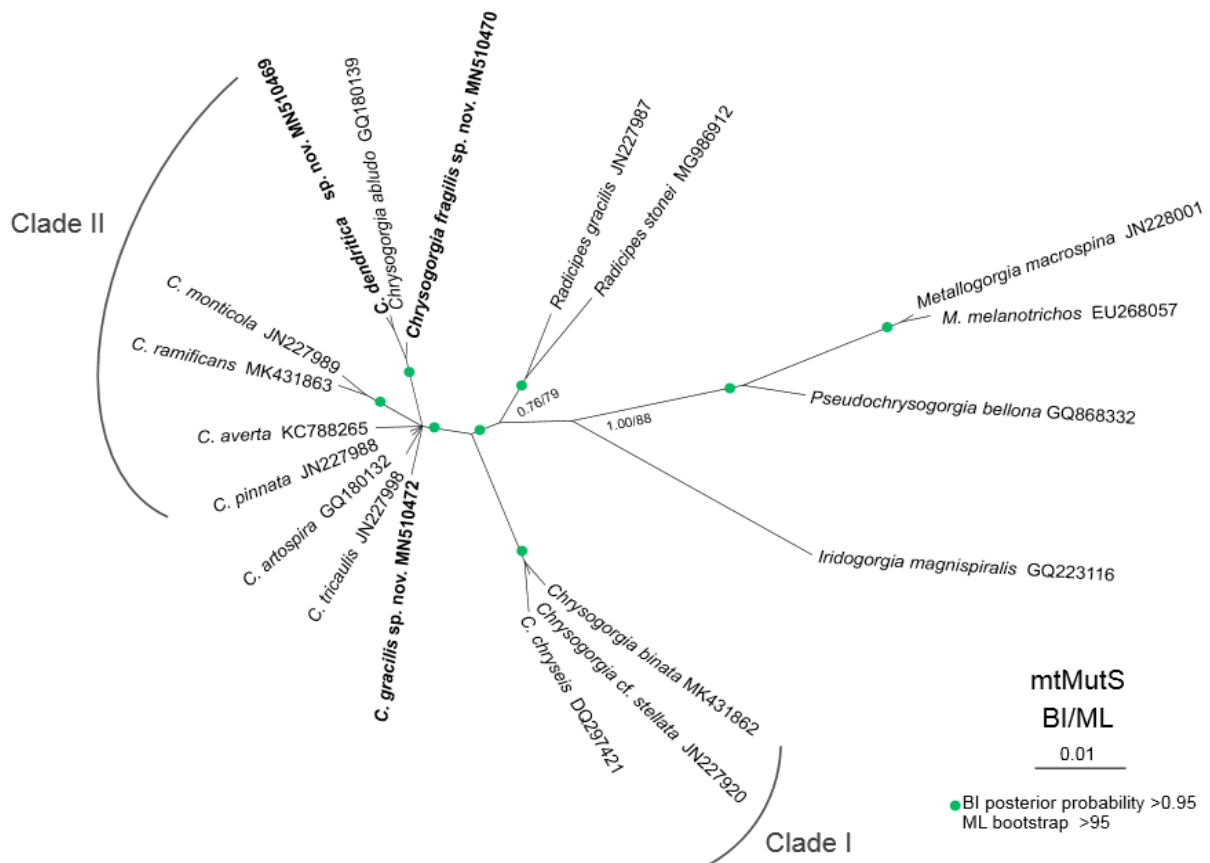
349

350 **Genetic distance and phylogenetic analyses**

351

352 The mtMutS sequences of the three new species were obtained and deposited in GenBank, with
353 the accession number and the length are as follows: MN510469, 620 bp for *Chrysogorgia*
354 *dendritica* sp. nov.; MN510470, 635 bp for *C. fragilis* sp. nov.; and MN510472, 635 bp for *C.*
355 *gracilis* sp. nov. The alignment dataset comprised 623 nucleotide positions. The present
356 intraspecific distances were calculated based on *C. abludo*, *C. tricaulis*, *C. artospira*, *C. averta*
357 and *C. chryseis* populations, and no intraspecific variability was observed for the four species
358 (Table 2). The mtMutS genetic distances among the species of *Chrysogorgia* range from zero to
359 2.42% (Table 2). The genetic distances between the new species *C. fragilis* sp. nov. and
360 congeners are in the range of 0.16%–2.26%, and those between *C. gracilis* sp. nov. and congeners
361 are in the range of 0.48%–2.10% (Table 2). No genetic variability was observed between
362 *dendritica* sp. nov. and *C. abludo*, and the genetic distances between this new species and the rest
363 congeners range from 0.16% to 2.42% (Table 2).

364 The ML and BI phylogenetic trees are identical in topology, and thus only the former with
365 the both support values was showed (Fig. 9). The *Chrysogorgia* species were separated into two
366 main clades (Clade I and II) with high support values. Clade I includes *C. binata*, *C. cf. stellata*
367 and *C. chryseis*, and Clade II contains all the rest species. The new species *C. dendritica* sp. nov.
368 and *C. abludo* formed a sister subclade, followed by *C. fragilis* sp. nov. *Chrysogorgia gracilis* sp.
369 nov. formed a sister subclade with *C. tricaulis*, *C. artospira*, *C. pinnata*, *C. averta* and the
370 subclade *C. ramificans* + *C. monticola*.



371

372 **Figure 9 Maximum likelihood (ML) tree inferred from the mtMutS sequences of**
 373 ***Chrysogorgia* and the related species sequences.** The Bayesian inference (BI) tree and the ML
 374 tree are identical in topology. Node support is as follows: BI posterior probability / ML bootstrap.
 375 Newly sequenced species are in bold.

376 **Table 2 Interspecific and intraspecific uncorrected pairwise distances at mtMutS of species**
 377 **of *Chrysogorgia*.**
 378

	1	2	3	4	5	6	7	8	9	10	11	12	13
1 <i>Chrysogorgia gracilis</i> sp. nov. MN510472	-												
2 <i>C. dendritica</i> sp. nov. MN510469	0.97 %	-											
3 <i>C. fragilis</i> sp. nov. MN510470	1.13 %	0.16 %	-										
4 <i>C. abludo</i> GQ180139, JN227999	0.97 %	0	0.16 %	0									
5 <i>C. tricaulis</i> JN227998, JN227990, JN227991, GQ180123-31, EU268056	0.65 %	0.97 %	0.81 %	0.97 %	0								
6 <i>C. artospira</i> GQ180132-5, GQ353317	0.48 %	0.81 %	0.65 %	0.81 %	0.16 %	0							
7 <i>C. pinnata</i> JN227988	0.48 %	0.81 %	0.65 %	0.81 %	0.16 %	0	-						
8 <i>C. averta</i> KC788265, GQ180136	0.81 %	1.13 %	0.97 %	1.13 %	0.48 %	0.32 %	0.32 %	0					
9 <i>C. ramificans</i> MK431863	1.13 %	1.45 %	1.29 %	1.45 %	0.81 %	0.65 %	0.65 %	0.97 %	-				
10 <i>C. monticola</i> JN227989	1.13 %	1.45 %	1.29 %	1.45 %	0.81 %	0.65 %	0.65 %	0.97 %	0.32 %	-			
11 <i>C. binata</i> MK431862	2.10 %	2.42 %	2.26 %	2.42 %	1.77 %	1.61 %	1.61 %	1.94 %	2.26 %	2.26 %	-		
12 <i>C. cf. stellata</i> JN227920	1.94 %	2.26 %	2.10 %	2.26 %	1.61 %	1.45 %	1.45 %	1.77 %	2.10 %	2.10 %	0.16 %	-	
13 <i>C. chryseis</i> JN227992, DQ297421	2.10 %	2.42 %	2.26 %	2.42 %	1.77 %	1.61 %	1.61 %	1.94 %	2.26 %	2.26 %	0.48 %	0.32 %	0

379 Discussion

380

381 Both the morphology and molecular phylogenetic analysis supported the assignment of the three
382 new species to the genus *Chrysogorgia*. The genetic distance analysis of mtMutS is considered as
383 one of the first steps in an integrative identification of octocorals ([McFadden et al., 2011](#); [Pante
384 et al., 2012, 2015](#)). In the present study, however, the mtMutS genetic distances within
385 *Chrysogorgia* are relatively low, and there is no barcoding gap (intraspecific zero vs. interspecific
386 0–2.42%) for species separation. Alternatively, single mutations on mtMutS, corresponding to the
387 genetic distance of ca. 0.16%, can be used to separate *Chrysogorgia* species ([Pante & Watling,
388 2012](#); [Pante et al., 2015](#); [this study](#)). *Chrysogorgia gracilis* sp. nov. and *C. fragilis* sp. nov.
389 showed at least one single mutation difference from congeners (the corresponding genetic
390 distances in range of 0.16%–2.26%; Table 2), supporting the establishment of the two new
391 species. Although no genetic variability was observed between *C. dendritica* sp. nov. and *C.
392 abludo*, the former is distinctly different from the latter by its unique monopodial stem and the
393 amoeba-shaped sclerites at the polyp body bases.

394 Based on the diagnosis sensu [Pante & Watling, 2012](#) and [Cordeiro et al., 2015](#), the genus
395 *Chrysogorgia* includes three branching forms: a single ascending spiral (clockwise or
396 counterclockwise), a fan (planar colony) and two fans emerging from a short main stem
397 (biflabellate colony). Based on the phylogenetic analysis, all the available *Chrysogorgia* species
398 could be separated into two groups (Clade I and II). All species in Clade I (*C. binata*, *C. cf.
399 stellata* and *C. chryseis*) have a bi- or multi-flabellate colony, as in the type species *C.
400 desbonni* Duchassaing & Michelotti, 1864. The other species of *Chrysogorgia* possessing either a
401 bottlebrush-shaped, a planar or a tree-shaped colony formed the Clade II with high support (Fig.
402 9). Furthermore, the genetic distances between Clade I and II are much higher than the intra-clade
403 ones of Clade I (1.45%–2.42% vs. 0–0.48%; Table 2). Likely, Clade II represents a new subgroup
404 of *Chrysogorgia* or even a new genus. However, only the sequences from 12 of 75 *Chrysogorgia*
405 species are available for the genetic analysis. Further integrated genetic and morphological
406 analyses are needed to verify this suggestion.

407 It is worth of note that all the new species possess a tree-shaped colony (monopodial,
408 sympodial), which represent a new colony form in *Chrysogorgia*. Such a colony occurs also in *C.
409 abludo* ([Pante & Watling, 2012](#)). Therefore, we add the tree-shaped colony to the diagnosis of the
410 genus. Here, we extend the diagnosis of *Chrysogorgia* on the basis of [Pante & Watling \(2012\)](#)
411 and [Cordeiro et al. \(2015\)](#): Colony branching usually sympodial, occasionally monopodial,
412 arising from a single ascending spiral (clockwise or counterclockwise, bottlebrush-shaped
413 colony), a fan (planar colony), two fans emerging from a short main stem (biflabellate colony), or
414 an unbranched main stem forming a tree-shaped colony. Axis with a metallic shine, dark to
415 golden in color. Branch subdivided dichotomously or pinnately. Most polyps relatively large to
416 the size of the branches they sit on, few in number and well separated from one another. Sclerites
417 in the form of spindles, rods and scales with little ornamentation.

418

419 Acknowledgements

420 We thank the assistance of the crew of R/V *KeXue* and ROV *FaXian* for sample collection. We
421 also thank Dr. Yang Li for comments on an early manuscript and Mr. Shaoqing Wang for taking

422 the photos on board.

423

424 **Additional Information and Declarations**

425 **Competing Interests**

426 The authors declare there are no competing interests.

427

428 **Author Contributions**

429 Yu Xu conceived and designed the experiments, performed the experiments, analyzed the
430 morphological data, prepared figures and tables, authored drafts of the paper, approved the final
431 draft.

432 Zifeng Zhan analyzed the molecular data, prepared figures and tables, authored drafts of the
433 paper, approved the final draft.

434 Kuidong Xu conceived and designed the experiments, reviewed drafts of the paper, approved the
435 final draft.

436

437 **Data Availability and DNA Deposition**

438 The following information was supplied regarding data availability:

439 The specimens described in this study are deposited in the Marine Biological Museum of Chinese
440 Academy of Sciences (MBMCAS) at Institute of Oceanology, Qingdao, China. Voucher ID
441 for *Chrysogorgia dendritica* is MBM286354; vouchers ID for the holotype and paratypes
442 of *Chrysogorgia fragilis* are MBM286351 and MBM286352, respectively; Voucher ID for
443 *Chrysogorgia gracilis* is MBM286350. The mtMuts sequences of the new species are available at
444 NCBI GenBank: MN510469, MN510470 and MN510472, respectively.

445

446 **New Species Registration**

447 The following information was supplied regarding the registration of a newly described species:
448 Publication LSID: urn:lsid:zoobank.org:pub:00D5E053-EFF8-4142-8D16-AAFC17D028E2.
449 *Chrysogorgia dendritica* sp. nov. LSID: urn:lsid:zoobank.org:act:F0050AD3-9E65-4B03-8D26-
450 2C687018DCAD, *Chrysogorgia fragilis* sp. nov. LSID: urn:lsid:zoobank.org:act:562CFDA7-
451 88F5-4D81-8FE5-BDE1F56A3EEC, and *Chrysogorgia gracilis* sp. nov. LSID:
452 urn:lsid:zoobank.org:act:F557CE43-D43C-4E5F-86C1-3EFE330A9443.

453

454 **Funding**

455 This work was supported by the Key Program of National Natural Science Foundation of China
456 (No. 41930533), the Strategic Priority Research Program of the Chinese Academy of Sciences
457 (XDA19060401), the Science & Technology Basic Resources Investigation Program of China
458 (2017FY100804) and the Senior User Project of RV KEXUE.

459

460 **References**

- 461 **Alfaro ME, Zoller S, Lutzoni F. 2003.** Bayes or Bootstrap? A simulation study comparing the
462 performance of Bayesian Markov chain Monte Carlo sampling and bootstrapping in
463 assessing phylogenetic confidence. *Molecular Biology and Evolution* **20**(2): 255–266.
- 464 **Bayer FM, Grasshoff M, Verseveldt J. 1983.** Illustrated Trilingual Glossary of Morphological
465 and Anatomical Terms Applied to Octocorallia. E. J. Brill/Dr. W. Backhuys, Leiden, 75 pp.
- 466 **Cairns SD. 2001.** Studies on western Atlantic Octocorallia (Gorgonacea: Ellisellidae). Part 1:
467 The genus *Chrysogorgia* Duchassaing & Michelotti, 1864. *Proceedings of the Biological*

- 468 *Society of Washington* **114**(3): 746–787.
469 [https://doi.org/10.2988/0006-324X\(2007\)120\[243:SOWAOG\]2.0.CO;2](https://doi.org/10.2988/0006-324X(2007)120[243:SOWAOG]2.0.CO;2)
- 470 **Cairns SD. 2018.** Deep-Water Octocorals (Cnidaria, Anthozoa) from the Galápagos and Cocos
471 Islands. Part 1: Suborder Calcaxonia. *ZooKeys* **729**: 1–46.
472 <https://doi.org/10.3897/zookeys.729.21779>
- 473 **Cordeiro RTS, Castro CB, Pérez CD. 2015.** Deep-water octocorals (Cnidaria: Octocorallia)
474 from Brazil: family Chrysogorgiidae Verrill, 1883. *Zootaxa* **4058**(1): 81–100.
475 <https://doi.org/10.11646/zootaxa.4058.1.4>
- 476 **Darriba D, Taboada GL, Doallo R, Posada D. 2012.** jModelTest 2: more models, new
477 heuristics and parallel computing. *Nature Methods* **9**: 772.
- 478 **Deichmann, E. 1936.** The Alcyonaria of the western part of the Atlantic Ocean. *Memoirs of the*
479 *Museum of Comparative Zoology, Harvard*, **53**, 1–317.
- 480 **Duchassaing P, Michelotti J. 1864.** Supplément au mémoire sur les coralliaires des Antilles.
481 *Memorie della Reale Accademia delle Scienze di Torino* **2**(23): 97–206
- 482 **Ehrenberg CG. 1834.** Beiträge zur physiologischen Kenntniss der Corallenthiere im
483 allgemeinen, und besonders des rothen Meeres, nebst einem Versuche zur physiologischen
484 Systematik derselben. *Abhandlungen der Königlichen Akademie der Wissenschaften, Berlin*
485 **1**: 225–380.
- 486 **Grasshoff M. 1999.** The shallow-water gorgonians of New Caledonia and adjacent islands
487 (Coelenterata, Octocorallia). *Senckenbergiana biologica* **78**: 1–121.
- 488 **Guindon S, Dufayard JF, Lefort V, Anisimova M, Hordijk W, Gascuel O. 2010.** New
489 algorithms and methods to estimate maximum-likelihood phylogenies: assessing the
490 performance of PhyML 3.0. *Systematic Biology* **59**: 307–321.
- 491 **Haeckel E. 1866.** Generelle morphologie der Organismen, vol. 2. Verlag von Georg Reimer,
492 Berlin.
- 493 **Herrera S, Baco A, Sánchez JA. 2010.** Molecular systematics of the bubblegum coral genera
494 (Paragorgiidae, Octocorallia) and description of a new deep-sea species. *Molecular*
495 *Phylogenetics and Evolution* **55**(1): 123–135.
- 496 **Hillis DM, Bull JJ. 1993.** An empirical test of bootstrapping as a method for assessing
497 confidence in phylogenetic analysis. *Systematic Biology* **42**(2): 182–192.
- 498 **Katoh K, Standley DM. 2013.** MAFFT Multiple Sequence Alignment Software version 7:
499 improvements in performance and usability. *Molecular Biology and Evolution* **30**: 772–780.
- 500 **Kinoshita K. 1913.** Studien über einige Chrysogorgiiden Japans. *Journal of the College of*
501 *Science, Tokyo Imperial University* **33**(2): 47 pp.
- 502 **Kükenthal, W. 1908.** Diagnosen neuer Gorgoniden aus der Gattung *Chrysogorgia* (6.
503 Mitteilung). *Zoologischer Anzeiger* **33**(21): 704–708.
- 504 **Lamouroux JVF. 1812.** Extrait d'un mémoire sur la classification des polypiers coralligènes non
505 entièrement pierreux. *Nouveau Bulletin des Sciences, Société Philomathique de Paris* **3**(63):
506 181–188.
- 507 **Yang Li, Zifeng Zhan, Kuidong Xu. 2017.** Morphology and molecular phylogeny of
508 *Paragorgia rubra* sp. nov. (Cnidaria: Octocorallia), a new bubblegum coral species from a

- 509 seamount in the tropical Western Pacific. *Chinese Journal of Oceanology and Limnology*
510 35(4): 803–814.
511 <http://dx.doi.org/10.1007/s00343-017-5320-5>
- 512 **McFadden CS, Benayahu Y, Pante E, Thoma JN, Nevarez PA, France SC. 2011.** Limitations
513 of mitochondrial gene barcoding in Octocorallia. *Molecular Ecology Resources* 11(1):19–
514 31.
- 515 **Pante E, France SC. 2010.** *Pseudochrysogorgia bellona* n. gen., sp. nov.: a new genus and
516 species of chrysogorgiid octocoral (Coelenterata, Anthozoa) from the Coral Sea. *Zoosystema*
517 32(4): 595–612.
518 <https://doi.org/10.5252/z2010n4a4>
- 519 **Pante E, Watling L. 2012.** *Chrysogorgia* from the New England and Corner Seamounts:
520 Atlantic–Pacific connections. *Journal of the Marine Biological Association of the United*
521 *Kingdom* 92(5): 911–927.
522 <http://doi.org/10.1017/S0025315411001354>
- 523 **Pante E, France SC, Couloux A, Cruaud C, McFadden CS, Samadi S, Watling L. 2012.**
524 Deep-sea origin and in-situ diversification of chrysogorgiid octocorals. *PLoS ONE* 7(6):
525 e38357.
- 526 **Pante E, Abdelkrim J, Viricel A, Gey D, France SC, Boisselier MC, Samadi S. 2015.** Use of
527 rad sequencing for delimiting species. *Heredity* 114: 450–459.
- 528 **Ronquist FR, Huelsenbeck JP. 2003.** MrBayes 3: Bayesian phylogenetic inference under mixed
529 models. *Bioinformatics* 19: 1572–1574.
- 530 **Sánchez JA, Lasker HR, Taylor DJ. 2003.** Phylogenetic analyses among octocorals (Cnidaria):
531 mitochondrial and nuclear DNA sequences (lsu-rRNA, 16S and ssu-rRNA, 18S) support two
532 convergent clades of branching gorgonians. *Molecular Biology and Evolution* 29: 31–42.
- 533 **Tamura K, Stecher G, Peterson D, Filipski A, Kumar S. 2013.** MEGA6: Molecular
534 Evolutionary Genetics Analysis Version 6.0. *Molecular Biology and Evolution* 30(12):
535 2725–2729.
- 536 **Verrill AE. 1883.** Report on the Anthozoa, and on some additional species dredged by the
537 "Blake" in 1877–1879, and by the U.S. Fish Commission steamer "Fish 126 Hawk" in
538 1880–82. *Bulletin of the Museum of Comparative Zoology* 11: 1–72.
- 539 **Versluys J. 1902.** Die Gorgoniden der Siboga-Expedition. 1. Die Chrysogorgiiden. *Siboga*
540 *Expeditie* 13: 1–120.
- 541 **Watling, L. 2007.** A review of the genus *Iridogorgia* (Octocorallia: Chrysogorgiidae) and its
542 relatives, chiefly from the North Atlantic Ocean. *Journal of the Marine Biological*
543 *Association of the UK* 87: 393–402.
- 544 **Yu Xu, Yang Li, Zifeng Zhan, Kuidong Xu. 2019.** Morphology and phylogenetic analysis of
545 two new deep-sea species of *Chrysogorgia* (Cnidaria, Octocorallia, Chrysogorgiidae) from
546 Kocebu Guyot (Magellan seamounts) in the Pacific Ocean. *Zookeys* 881: 91–107.
547 <https://doi.org/10.3897/zookeys.881.34759>

Table 1 (on next page)

Morphological comparisons between *C. averta*, *C. abludo*, *C. dendritica* sp. nov., *C. fragilis* sp. nov. and *C. gracilis* sp. nov.

1 **Table 1 Morphological comparisons between *C. averta*, *C. abludo*, *C. dendritica* sp. nov., *C.*
 2 *fragilis* sp. nov. and *C. gracilis* sp. nov.**

Characters/species	<i>C. averta</i>	<i>C. abludo</i>	<i>C. fragilis</i> sp. nov.	<i>C. dendritica</i> sp. nov.	<i>C. gracilis</i> sp. nov.
Group type	A	A	A	A	A
Colony shape	bottlebrush-shaped	tree-shaped	tree-shaped	tree-shaped	tree-shaped
Branching sequence	3/8L	1/3, 1/4L, irregular	1/3L	1/3L	1/4L
Interbranch distance (mm)	9–13	4.3–15.0	15–22	16–22	2.0–4.5
Orthostiche interval (mm)	75–78	No data	50–65	50–55	11-16
First branch internode (mm)	13–19	6.1–16.0	15–22	15–20	3-7
Polyps on internodes	0–2	1–2	0–4	1–5	1-10
Polyps on terminal branchlets	1–3	1–6	1–10	1–6	3–20
Polyps height (mm)	1.1–1.9	0.8–2.2	2.0–4.0	3.0	0.9-1.5
Sclerites in coenenchyme (µm)	rods and scales	small rugged scales	elongate skateboard-shaped scales	flat and lobed scales	elongated scales with smooth surface and edges
Sclerites in body wall (µm)	scales and rods	scales and rods	scales, rods and spindles	scales, rods and spindles	scales and rods
Sclerites in tentacles (µm)	rods	rods	rods	rods	scales and rods
Distribution	North Atlantic	North Atlantic	Western Pacific	Western Pacific	Western Pacific
References	Pante & Watling 2012	Pante & Watling 2012	Present study	Present study	Present study

3

4

Table 2 (on next page)

Interspecific and intraspecific uncorrected pairwise distances at mtMutS of species of *Chrysogorgia*

1 **Table 2 Interspecific and intraspecific uncorrected pairwise distances at mtMutS of species of *Chrysogorgia*.**

2

	1	2	3	4	5	6	7	8	9	10	11	12	13	
<i>Chrysogorgia gracilis</i> sp. nov.														
1	MN510472	-												
2	<i>C. dendritica</i> sp. nov. MN510469	0.97%	-											
3	<i>C. fragilis</i> sp. nov. MN510470	1.13%	0.16%	-										
4	<i>C. abludo</i> GQ180139, JN227999	0.97%	0	0.16%	0									
5	<i>C. tricaulis</i> JN227998, JN227990, JN227991, GQ180123-31, EU268056	0.65%	0.97%	0.81%	0.97%	0								
6	<i>C. artospira</i> GQ180132-5, GQ353317	0.48%	0.81%	0.65%	0.81%	0.16%	0							
7	<i>C. pinnata</i> JN227988	0.48%	0.81%	0.65%	0.81%	0.16%	0	-						
8	<i>C. averta</i> KC788265, GQ180136	0.81%	1.13%	0.97%	1.13%	0.48%	0.32%	0.32%	0					
9	<i>C. ramificans</i> MK431863	1.13%	1.45%	1.29%	1.45%	0.81%	0.65%	0.65%	0.97%	-				
10	<i>C. monticola</i> JN227989	1.13%	1.45%	1.29%	1.45%	0.81%	0.65%	0.65%	0.97%	0.32%	-			
11	<i>C. binata</i> MK431862	2.10%	2.42%	2.26%	2.42%	1.77%	1.61%	1.61%	1.94%	2.26%	2.26%	-		
12	<i>C. cf. stellata</i> JN227920	1.94%	2.26%	2.10%	2.26%	1.61%	1.45%	1.45%	1.77%	2.10%	2.10%	0.16%	-	
13	<i>C. chryseis</i> JN227992, DQ297421	2.10%	2.42%	2.26%	2.42%	1.77%	1.61%	1.61%	1.94%	2.26%	2.26%	0.48%	0.32%	0

3

Figure 1

Sampling sites on a seamount (M2) adjacent to the Mariana Trench and the Kocebu Guyot in the Western Pacific Ocean.

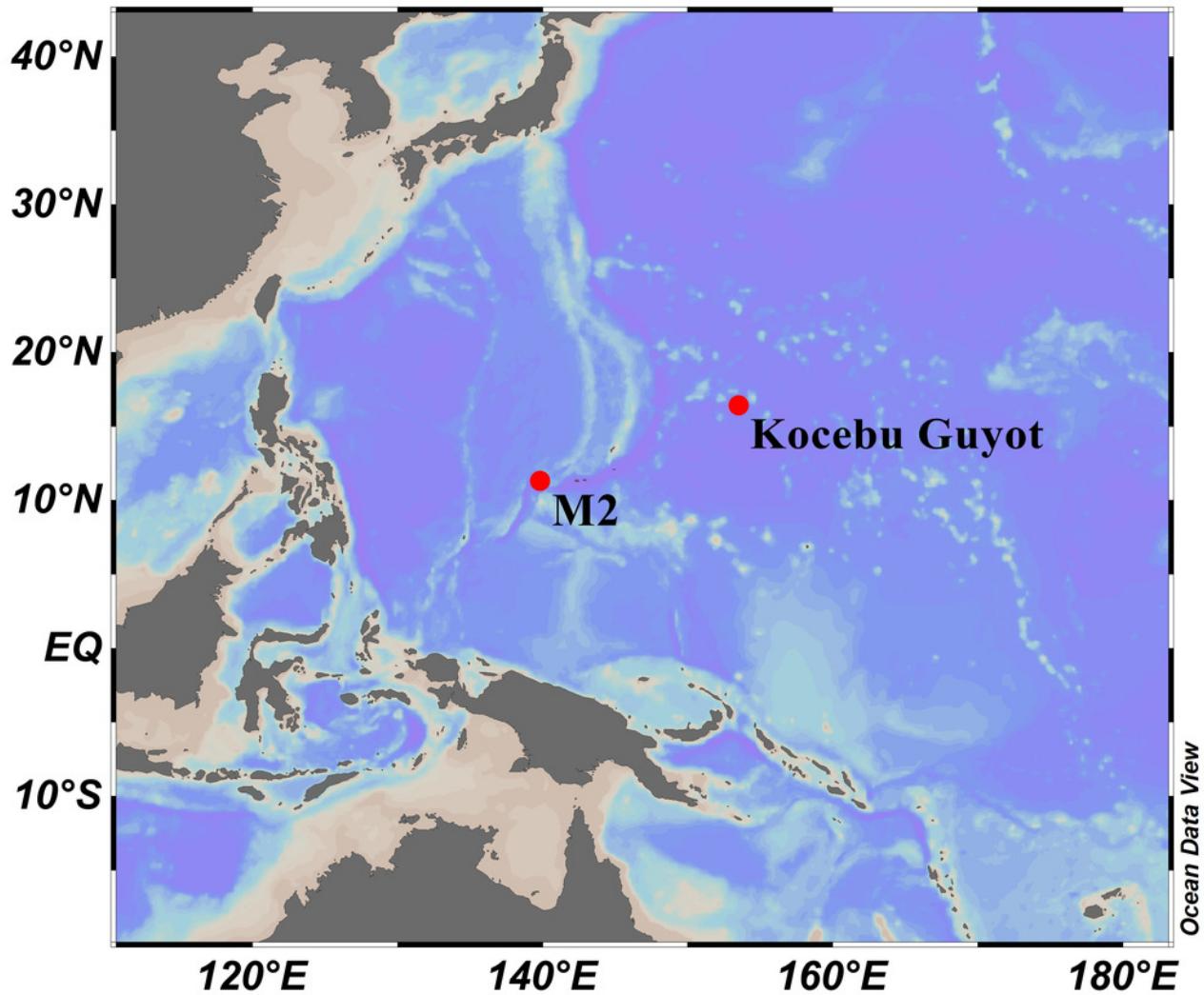


Figure 2

The external morphology and polyps of *Chrysogorgia dendritica* sp. nov.

(A) The holotype *in situ*; (B) The holotype immediately after collection; (C) A single polyp under light microscope; (D) Single polyp under SEM. Scale bars: 10 cm (B); 1 mm (C, D).

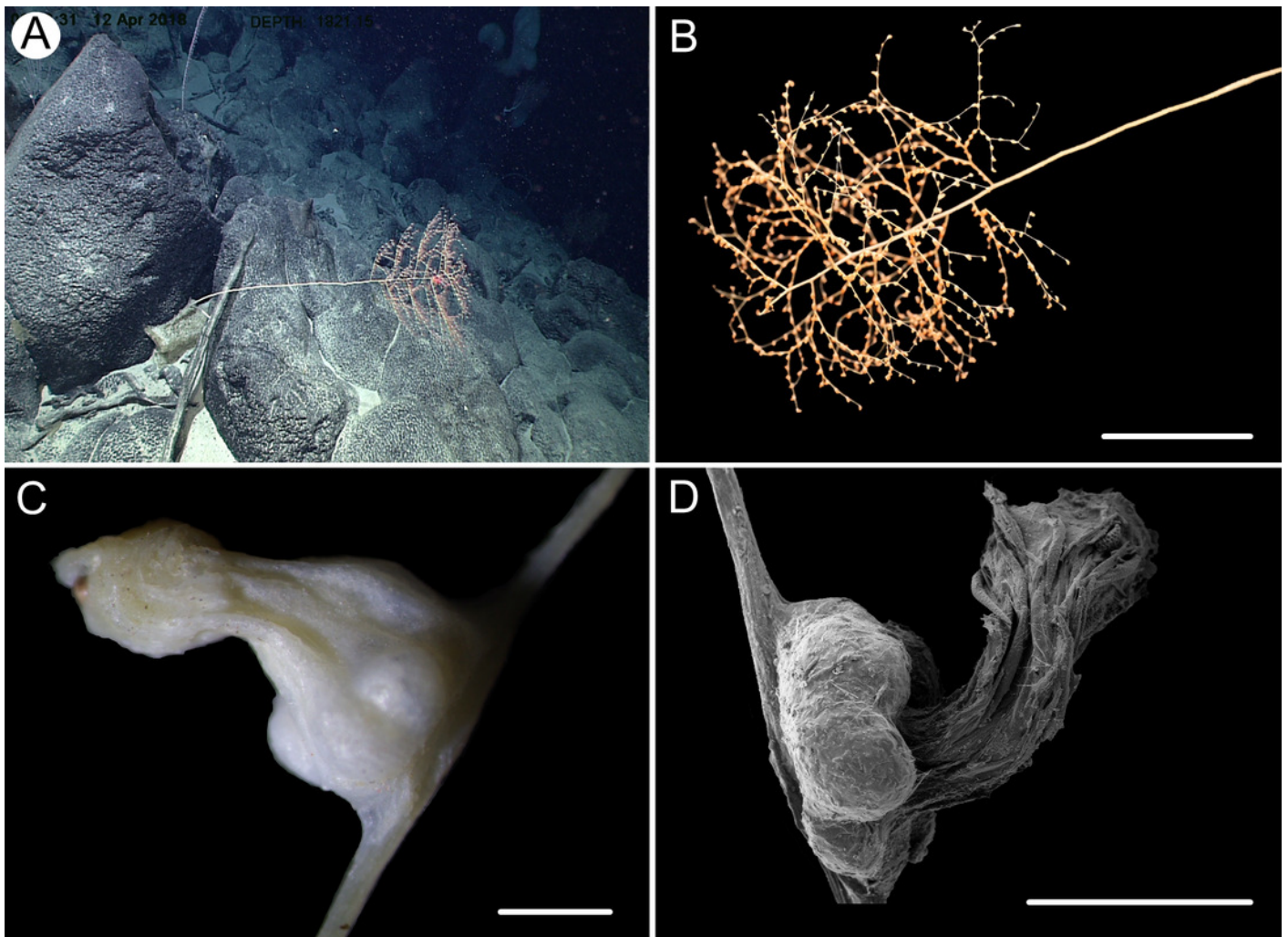


Figure 3

Polyps and branches of *Chrysogorgia dendritica* sp. nov. under SEM.

(A) A terminal polyp and a middle polyp; (B) The tentacles with rods; (C) The basal body with scales; (D) The neck with rods and spindles; (E) The coenenchyme with scales. Scale bars: 1 mm (A); 500 μ m (B-E at the same scale).

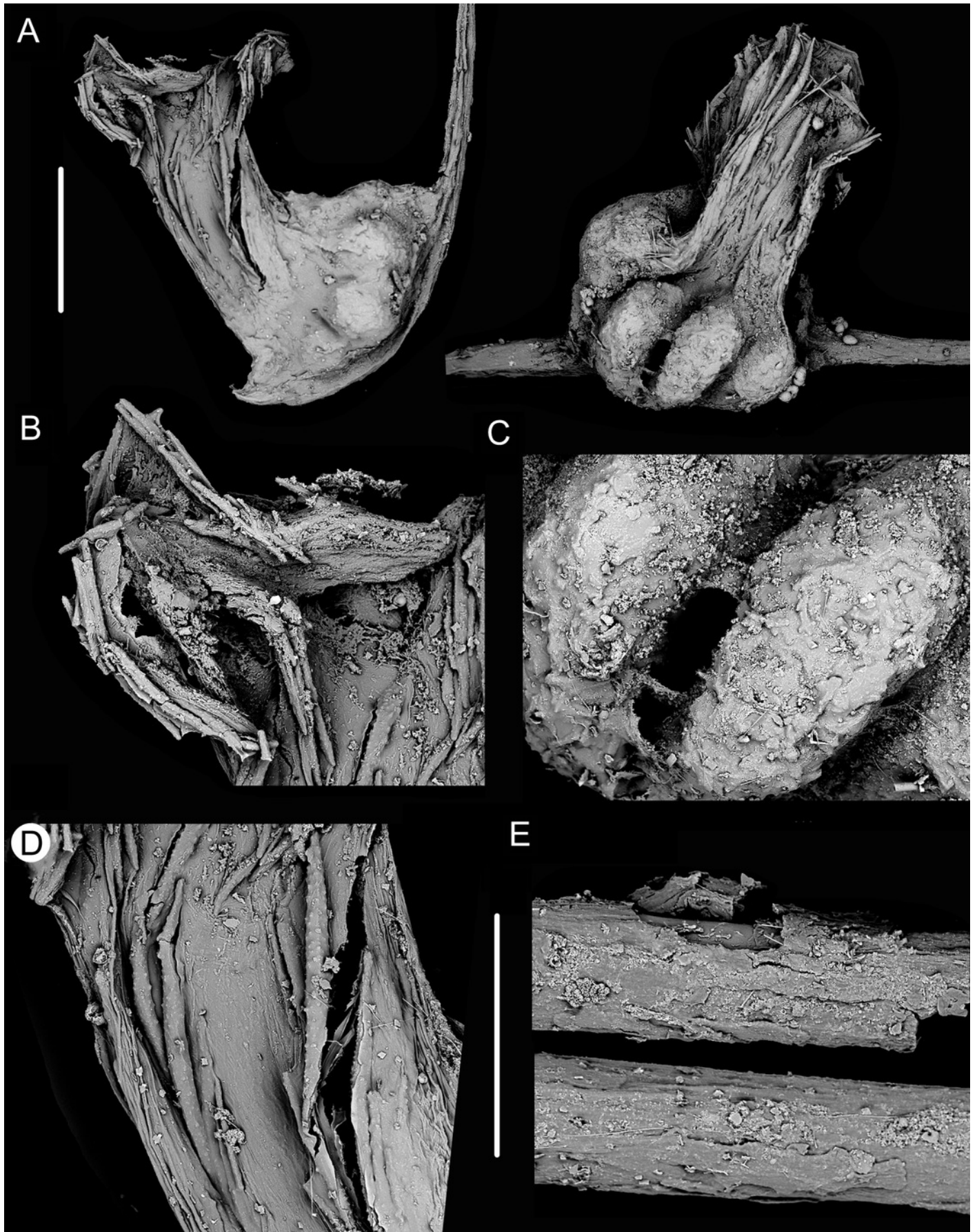


Figure 4

Sclerites of *Chrysogorgia dendritica* sp. nov.

(A) Sclerites of the polyp neck and tentacles; (B) Sclerites at the body base; (C) Sclerites in coenenchyme. Scale bars: 200 μm (A), 100 μm (B, C, at the same scale).



Figure 5

The external morphology and polyps of *Chrysogorgia fragilis* sp. nov.

(A) The holotype *in situ*. Laser dots spaced at 33 cm used for measuring dimensions; (B) The paratype *in situ*; (C) The holotype immediately after collection; (D) The paratype after fixation; (E) A single polyp under light microscope; (F) A single polyp under SEM. Scales bars: 10 cm (C, D); 1 mm (E, F).

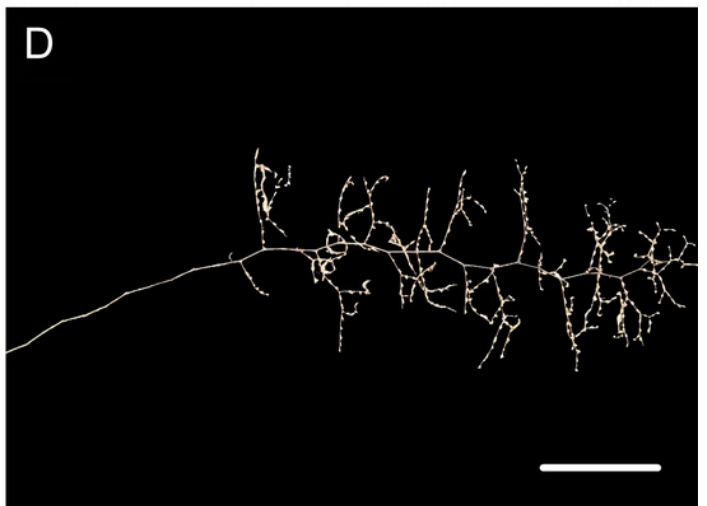
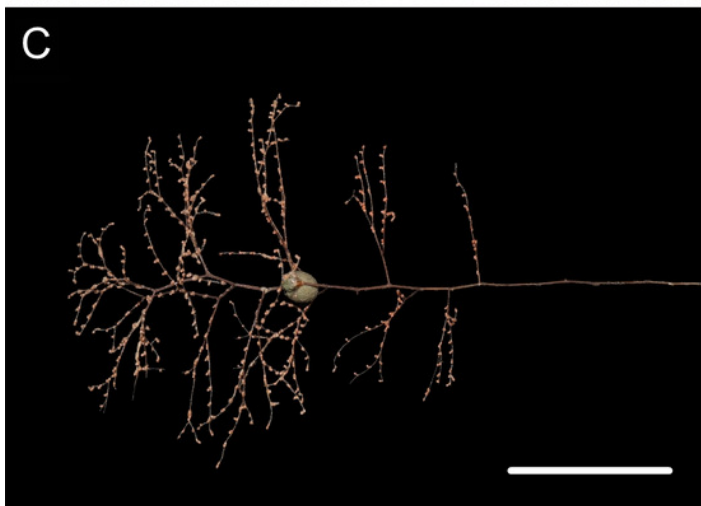
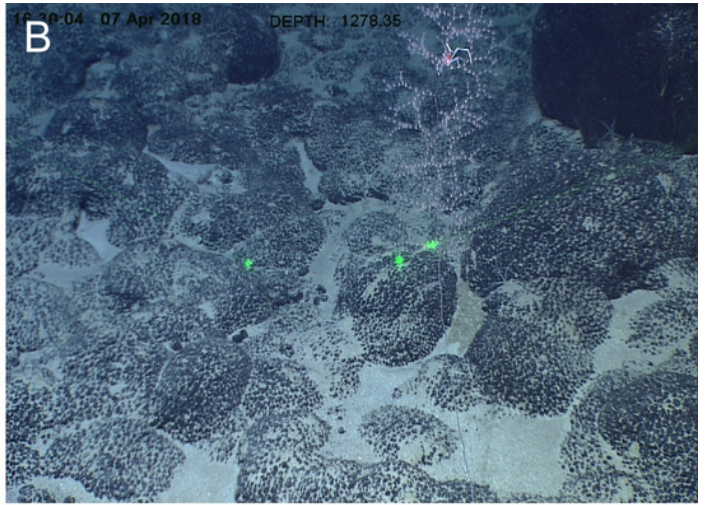


Figure 6

Sclerites of *Chrysogorgia fragilis* sp. nov.

(A) Sclerites of the polyp neck and tentacles; (B) Sclerites at the expanded polyp body base; (C) Sclerites in coenenchyme. Scale bar: 200 μm (all at the same scale).

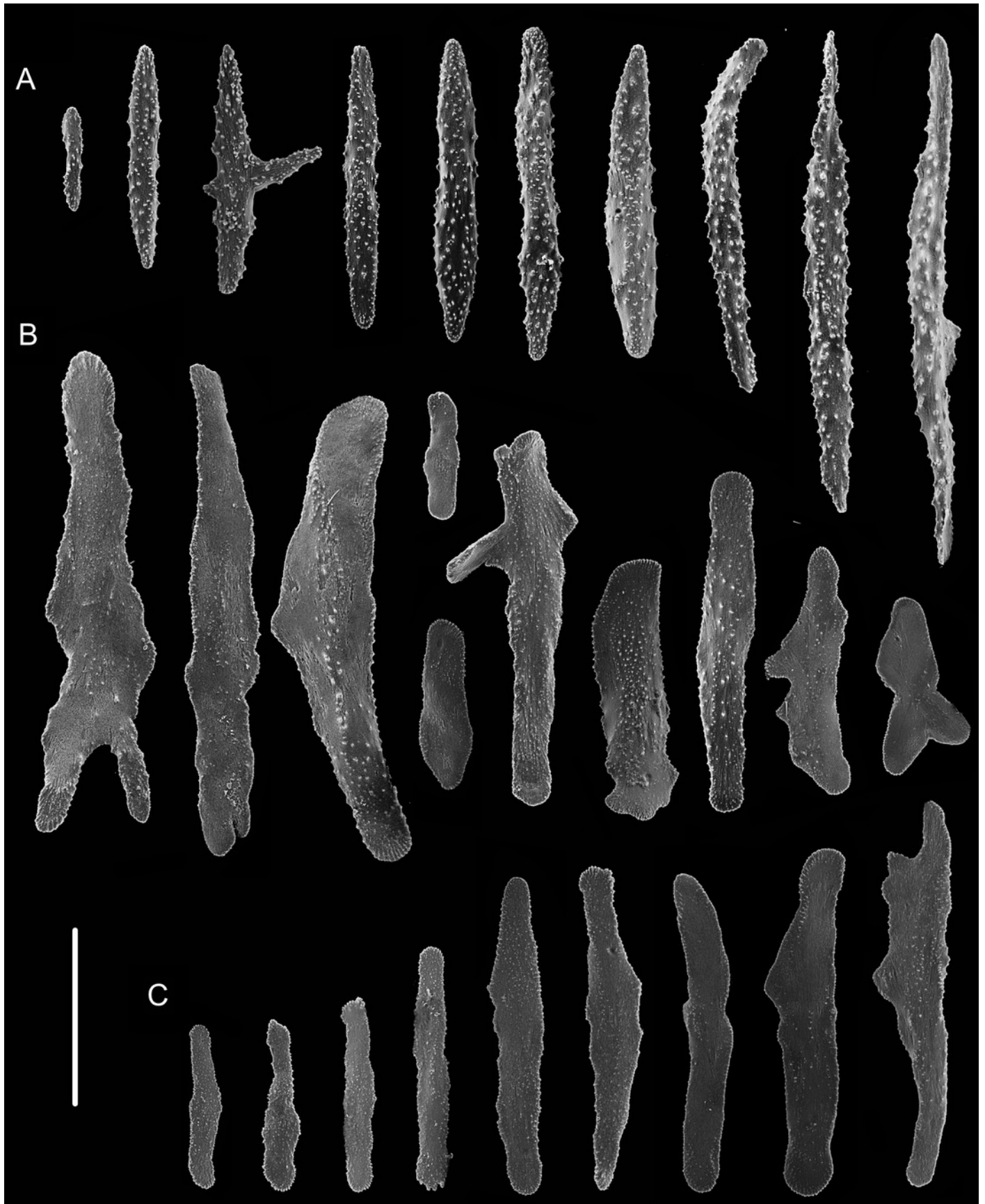


Figure 7

The external morphology and polyps of the holotype of *Chrysogorgia gracilis* sp. nov.

(A-C) The holotype *in situ* (A) and after collection (B) and fixation (C); Laser dots spaced at 33 cm used for measuring dimensions; (D) A single polyp under light microscope; (E) A single polyp under SEM; (F) Tentacles under SEM; (G) Mesozooids at the base of branch under light microscope; (H) Four mesozooids under SEM; (I) A single mesozooid under SEM. Scales bars: 5cm (C), 300 μ m (D-I).

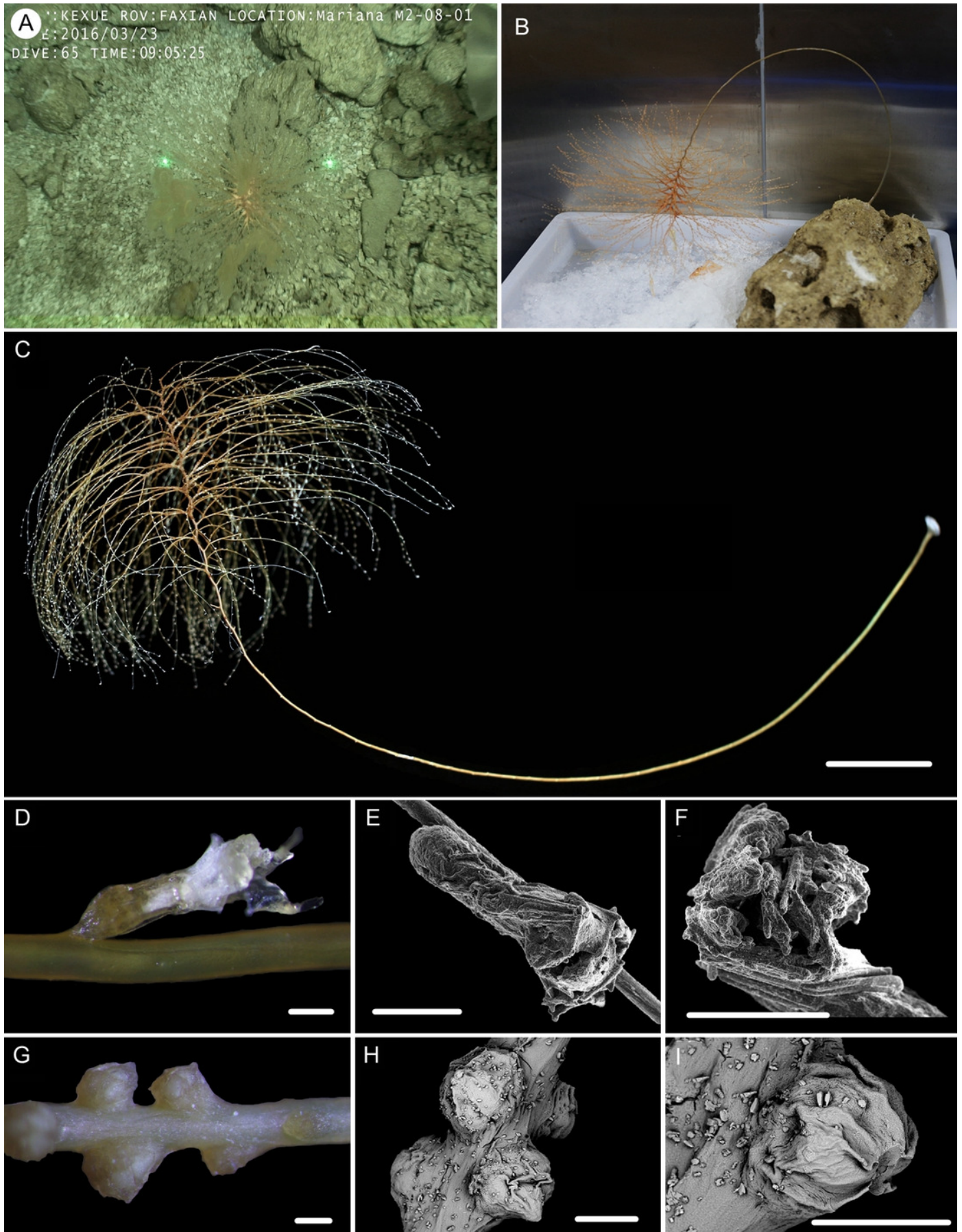


Figure 8

Sclerites of *Chrysogorgia gracilis* sp. nov.

(A) Sclerites in tentacles and at the bases of tentacles; (B) Sclerites in coenenchyme. Scales bars: 100 μ m (all at the same scale).

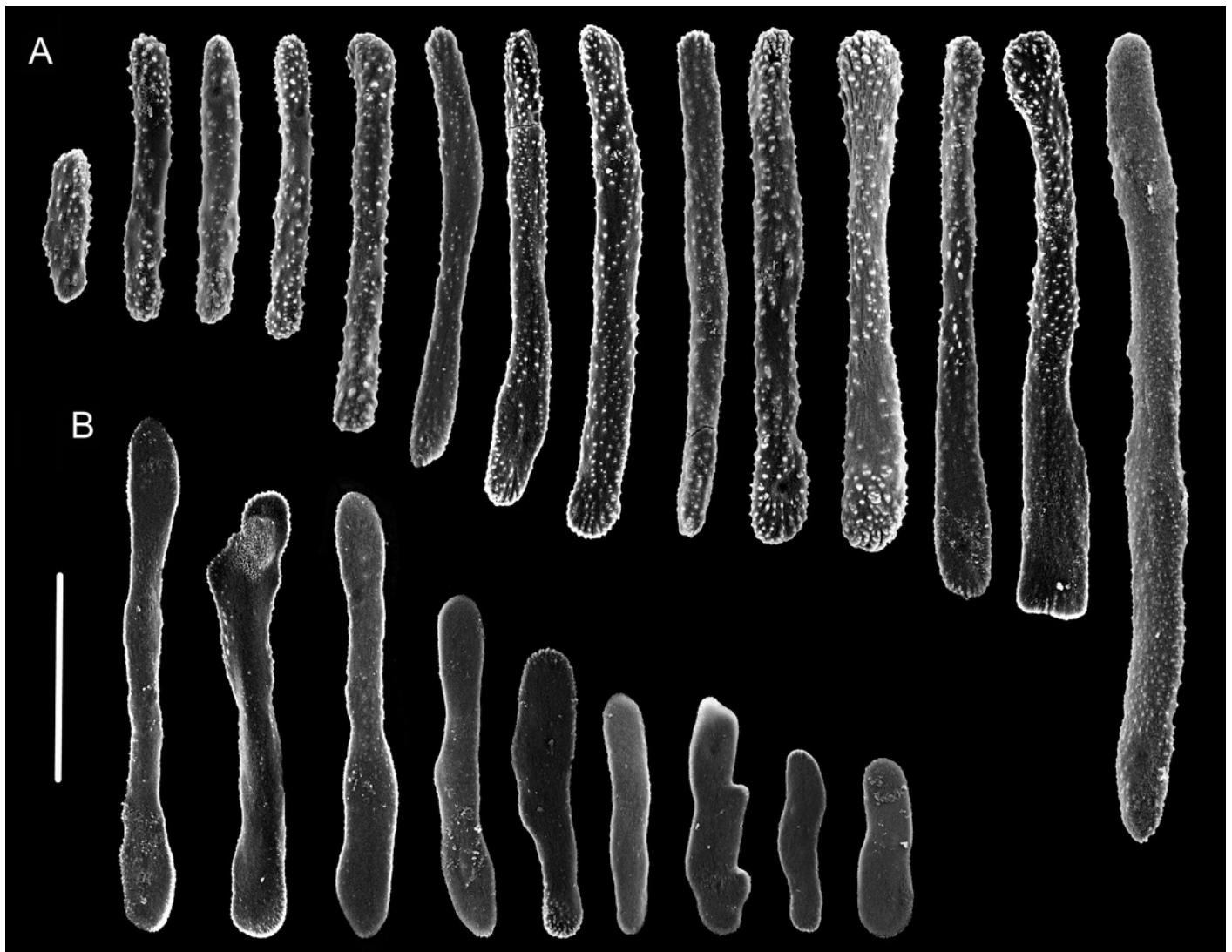


Figure 9

Maximum likelihood (ML) tree inferred from the mtMutS sequences of *Chrysogorgia* and the related species sequences.

The Bayesian inference (BI) tree and the ML tree are identical in topology. Node support is as follows: BI posterior probability / ML bootstrap. Newly sequenced species are in bold.

